© 2016. Published by The Company of Biologists Ltd | Journal of Cell Science (2016) 129, 2394-2406 doi:10.1242/jcs.186148

RESEARCH ARTICLE

# The *O*-glycosylated ectodomain of FXYD5 impairs adhesion by disrupting cell–cell trans-dimerization of Na,K-ATPase $\beta_1$ subunits

**Elmira Tokhtaeva[1,2], Haying Sun[3], Nimrod Deiss-Yehiely[3], Yi Wen[1,2], Pritin N. Soni[3], Nieves M. Gabrielli[3,4], Elizabeth A. Marcus[2,5], Karen M. Ridge[3], George Sachs[1,2], Mónica Vazquez-Levin[4], Jacob I. Sznajder[3], Olga Vagin[1,2] and Laura A. Dada[3,*]**

## ABSTRACT

FXYD5 (also known as dysadherin), a regulatory subunit of the Na,K-ATPase, impairs intercellular adhesion by a poorly understood mechanism. Here, we determined whether FXYD5 disrupts the trans-dimerization of Na,K-ATPase molecules located in neighboring cells. Mutagenesis of the Na,K-ATPase $\beta_1$ subunit identified four conserved residues, including Y199, that are crucial for the intercellular Na,K-ATPase trans-dimerization and adhesion. Modulation of expression of FXYD5 or of the $\beta_1$ subunit with intact or mutated $\beta_1$–$\beta_1$ binding sites demonstrated that the anti-adhesive effect of FXYD5 depends on the presence of Y199 in the $\beta_1$ subunit. Immunodetection of the plasma membrane FXYD5 was prevented by the presence of *O*-glycans. Partial FXYD5 deglycosylation enabled antibody binding and showed that the protein level and the degree of *O*-glycosylation were greater in cancer than in normal cells. FXYD5-induced impairment of adhesion was abolished by both genetic and pharmacological inhibition of FXYD5 *O*-glycosylation. Therefore, the extracellular *O*-glycosylated domain of FXYD5 impairs adhesion by interfering with intercellular $\beta_1$–$\beta_1$ interactions, suggesting that the ratio between FXYD5 and $\alpha_1$–$\beta_1$ heterodimer determines whether the Na,K-ATPase acts as a positive or negative regulator of intercellular adhesion.

**KEY WORDS: Na,K-ATPase, Epithelium, Epithelial cell adhesion molecule, Cell–cell interaction, Cell adhesion, *O*-glycosylation, FXYD5**

## INTRODUCTION

The Na,K-ATPase plays a crucial role in epithelia by generating ion gradients and driving transepithelial $Na^+$-dependent transport of various solutes and water. In the alveolar epithelium, these gradients are responsible for water reabsorption from alveolar spaces, which is crucial for normal gas exchange (Mutlu and Sznajder, 2005; Sznajder, 2001; Vádasz et al., 2007). The two Na,K-ATPase subunits, a catalytic α subunit and an *N*-glycosylated structural β subunit are required for normal maturation, membrane targeting and transport activity of the enzyme (Barwe et al., 2012; Geering, 2001; Rajasekaran et al., 2001; Tokhtaeva et al., 2009). Additional regulatory subunits that are not obligatory for activity belong to a family of proteins that share an extracellular FXYD sequence (Geering, 2006; Miller and Davis, 2008; Sweadner and Rael, 2000). In mammals, seven members of the FXYD family are expressed, mostly in a tissue-specific manner, and associate with the Na,K-ATPase α–β heterodimer, modulating its activity (Garty and Karlish, 2006; Geering, 2006).

FXYD5 (also called dysadherin) is a type 1 transmembrane protein that contains a putative signal sequence, followed by an extracellular domain, a single trans-membrane domain, and a short cytoplasmic tail (Lubarski et al., 2005). As with other FXYD proteins, FXYD5 interacts with the Na,K-ATPase α-β heterodimer and regulates its activity by increasing the maximal velocity (Lubarski et al., 2005). FXYD5 is unique in the FXYD family as it possesses an extended extracellular *O*-glycosylated domain (Ino et al., 2002; Tsuiji et al., 2003). Elevated levels of FXYD5 in tumors of patients with different types of cancer correlate with a poor prognosis (Lee et al., 2012; Maehata et al., 2011; Mitselou et al., 2010; Park et al., 2011; Shimada et al., 2004), and overexpression of FXYD5 in various cell types results in the impairment of intercellular adhesion (Ino et al., 2002; Lubarski et al., 2011; Shimamura et al., 2004; Tsuiji et al., 2003). It has been suggested that overexpression of FXYD5 downregulates E-cadherin levels, promoting metastasis (Batistatou et al., 2007a; Ino et al., 2002; Shimamura et al., 2004; Tamura et al., 2005). However, E-cadherin-independent mechanisms have been also described, including the activation of the NF-κB pathway, leading to increased production of the tumor-promoting chemokine CCL2 (Lubarski et al., 2011; Nam et al., 2007; Park et al., 2011; Stamatovic et al., 2009). Moreover, FXYD5 is expressed in normal lung, kidney and gut epithelium (Lubarski et al., 2005), although the functional role of this protein in normal tissues is unclear.

In contrast to FXYD5, the Na,K-ATPase α–β heterodimer contributes to the formation and stabilization of intercellular junctions in epithelia (Cereijido et al., 2012; Rajasekaran and Rajasekaran, 2009; Vagin et al., 2012). It acts as a cell adhesion molecule by undergoing both intercellular trans-dimerization through its $\beta_1$ subunit and intracellular association with the cytoskeleton through its $\alpha_1$ subunit (Clifford and Kaplan, 2008; Shoshani et al., 2005). *N*-glycosylation of the $\beta_1$ subunit is important for normal cell adhesion because MDCK cells (a cell line with characteristics of the distal renal tubule) expressing the unglycosylated $\beta_1$ subunit form cell–cell contacts more slowly than non-transfected MDCK cells (Vagin et al., 2006, 2008). In addition, modulation of the structure of the Na,K-ATPase $\beta_1$ subunit *N*-glycans alters the stability of epithelial junctional complexes and paracellular permeability (Vagin et al., 2008), suggesting a role for the $\beta_1$ subunit *N*-glycans in regulation of cell adhesion. Both the

[1]Department of Physiology, David Geffen School of Medicine, UCLA, Los Angeles, CA 90095, USA. [2]Veterans Administration Greater Los Angeles Healthcare System, Los Angeles, CA 90095, USA. [3]Division of Pulmonary and Critical Care Medicine, Feinberg School of Medicine, Northwestern University, Chicago, IL 60611, USA. [4]Instituto de Biología y Medicina Experimental (CONICET-FIBYME), Buenos Aires C1418ADN, Argentina. [5]Department of Pediatrics, David Geffen School of Medicine, UCLA, Los Angeles, CA 90095, USA.

*Author for correspondence (lauradada@northwestern.edu)

N.M.G., 0000-0002-3270-9140; L.A.D., 0000-0003-0474-718X

**Received 20 January 2016; Accepted 26 April 2016**

Journal of Cell Science (2016) 129, 2394-2406 doi:10.1242/jcs.186148

facilitating role of the $\alpha_1$–$\beta_1$ heterodimers and the disrupting role of FXYD5 in cell adhesion are independent of the Na,K-ATPase activity (Balasubramaniam et al., 2015; Barwe et al., 2007; Lubarski et al., 2007, 2005; Vagin et al., 2006). It has previously been shown that the presence of FXYD5 alters the degree of *N*-glycosylation of the Na,K-ATPase $\beta_1$ subunit (Lubarski et al., 2011, 2005). The authors hypothesized that these changes might be responsible for the effects of FXYD5 on intercellular adhesion (Lubarski et al., 2011).

The 197–208 amino acid sequence in the extracellular domain of the $\beta_1$ subunit that is exposed toward a neighboring cell is involved in both $\beta_1$–$\beta_1$ interaction and intercellular adhesion (Tokhtaeva et al., 2012). Here, by site-directed mutagenesis, we have identified four conserved amino acid residues in this sequence that are responsible for the interaction between the Na,K-ATPase $\beta_1$ subunits, and used a mutant $\beta_1$ subunit that is unable to form $\beta_1$–$\beta_1$ bridges as a tool to investigate whether FXYD5 impairs intercellular adhesion by disrupting these bridges. Further, by modulating the FXYD5 level of expression or its degree of *O*-glycosylation in epithelial cells, we analyzed the role of FXYD *O*-glycans in intercellular adhesion. The results indicate that the extracellular *O*-glycosylated domain of FXYD5 impairs cell adhesion by preventing intercellular trans-dimerization of the Na,K-ATPase molecules through their $\beta_1$ subunits.

## RESULTS

### The *O*-glycosylated form of FXYD5 is expressed at the plasma membrane in normal and cancer epithelial cells

To study the effect of FXYD5 on intercellular adhesion, we used primary human and rat alveolar epithelial type II (ATII) cells, as well as A549, MDCK and HGE-20 cell lines. Human lung cancer A549 cells show many characteristics of ATII cells (Lieber et al., 1976), including the regulation of the Na,K-ATPase (Bertorello et al., 2003; Dada et al., 2003; Lecuona et al., 2006) but do not form tight epithelial monolayers, whereas canine renal epithelial MDCK cells and human gastric epithelial HGE-20 cells form tight junctions. Western blot analysis using two different antibodies against human FXYD5 detected a major band at ~32 kDa in A549, human ATII (hATII), MDCK and HGE-20 cell lysates (Fig. 1A). This band disappeared after transfecting A549 cells with FXYD5-specific small interfering RNA (siRNA) (Fig. 1A), indicating the

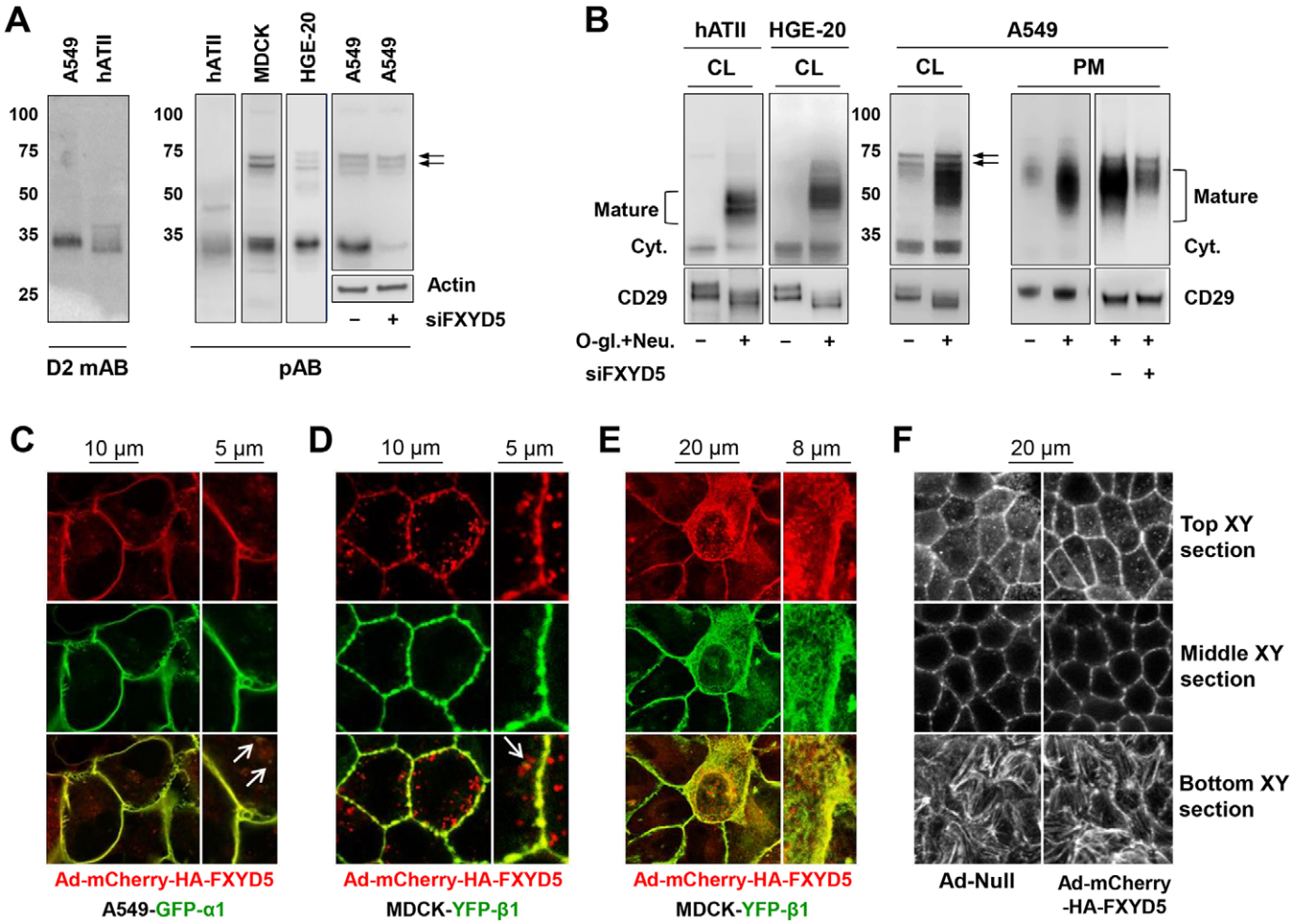


**Fig. 1. FXYD5 is expressed at the plasma membrane in cancer and normal epithelial cells.** (A) Cell lysates were analyzed by western blotting with FXYD5 D2 monoclonal (mAB) and polyclonal (pAB) antibodies. Where indicated, A549 cells were transfected with either scrambled siRNA (–) or FXYD5-specific siRNA (+). (B) Total cell lysates (CL) or plasma membrane (PM) proteins were treated with glycosidases (O-gl+Neu.) and analyzed by western blotting using FXYD5-specific antibody. CD29 was used as a control for glycosidase action. Cyt., cytosolic FXYD5. The arrows in A and B indicate non-specific bands. (C–E) A549-GFP$\alpha_1$ and MDCK-YFP-$\beta_1$ cells were infected with Ad-mCherry-HA-FXYD5 and analyzed by confocal microscopy. (F) MDCK-YFP-$\beta_1$ cells were infected as in C–E, and actin filaments were visualized. Representative blots or images from three independent experiments are shown. Arrows in C and D indicate intracellular colocalization of FXYD5 and Na,K-ATPase subunits.

Journal of Cell Science (2016) 129, 2394-2406 doi:10.1242/jcs.186148

specificity of the signal. The intensity of this band was greater in A549 than in hATII cells, consistent with previous reports on higher expression of FXYD5 in cancer cells (Ino et al., 2002; Nam et al., 2007). In addition, faint bands at 65–70 kDa were detected in A549, HGE-20 and MDCK cell lysates with a polyclonal antibody (Fig. 1A). These bands were not sensitive to FXYD5-specific siRNA (Fig. 1A, arrows) and, hence, apparently reflect a non-specific interaction of the antibody with other cellular proteins.

The extracellular domain of FXYD5 contains multiple sites of mucin-type GalNAc *O*-glycosylation, but the data on their extent and structure are controversial (Ino et al., 2002; Lubarski et al., 2011). To determine the presence of *O*-glycans in FXYD5, we treated cellular or surface proteins with a mixture of *O*-glycosidase and neuraminidase, which remove some but not all mucin-type *O*-glycans from glycoproteins (Fujikura et al., 2011). CD29 (β1 integrin), which is an *N*- and *O*-glycosylated protein (Clément et al., 2004; Lee et al., 2009), was used as the control for the glycosidase treatment (Fig. 1B). Western blot analysis of FXYD5 after glycosidase treatment revealed the appearance of diffuse bands of ∼40–50 kDa and of ∼45–55 kDa in hATII and HGE-20 cell lysates, respectively, and of ∼40–70 kDa in lysates and plasma membrane fraction of A549 cells (Fig. 1B). The level of FXYD5 in the plasma membrane of glycosidase-treated A549 cells was drastically decreased by FXYD5-specific siRNA (Fig. 1B). These results demonstrate that FXYD5 is heavily *O*-glycosylated in cancer and normal epithelial cells, but the extent of *O*-glycosylation is greater in cancer cells. Extensively glycosylated forms were hardly seen in untreated cells, suggesting that *O*-glycans interfere with the interaction between the mature FXYD5 and the anti-FXYD5 antibody. As expected, glycosidases had no effect on non-specific bands in A549 cells (Fig. 1B, arrows) or the 32-kDa band (Fig. 1B), suggesting that this intracellular fraction of FXYD5 contains *O*-glycosidase-resistant oligosaccharides or has other post-translational modifications. In glycosidase-treated cell lysates, the density of the extensively *O*-glycosylated fraction of FXYD5 was much greater than that of the intracellular 32-kDa fraction. In agreement with these results, FXYD5 was predominantly seen at the plasma membrane where it colocalized with the Na,K-ATPase in A549 cells expressing GFP-tagged $\alpha_1$ (A549-GFP–$\alpha_1$) (Fig. 1C) or in MDCK cells expressing YFP-tagged $\beta_1$ (MDCK-YFP–$\beta_1$) (Fig. 1D,E) after infection with mCherry–HA-tagged FXYD5 adenovirus (Ad-FXYD5). A partial intracellular colocalization of FXYD5 with the $\beta_1$ subunit apparently in the endoplasmic reticulum (ER) was seen in sub-confluent MDCK-YFP–$\beta_1$ cells (Fig. 1E). Very little intracellular colocalization of FXYD5 was seen with the Na,K-ATPase $\alpha_1$ or $\beta_1$ subunit in confluent A549 or MDCK cells (Fig. 1C,D, arrows). Overexpression of FXYD5 in MDCK cells did not alter the cell morphology or F-actin staining (Fig. 1F).

These results indicate the presence of multiple mucin-type *O*-glycans in the mature plasmalemma-resident FXYD5. In addition, these data demonstrate that this form of FXYD5, rather than its immature intracellular form, represents the major cellular pool of FXYD5.

### FXYD5 knockdown in cancer cells improves intercellular adhesion by allowing the intercellular $\beta_1$–$\beta_1$ interactions

FXYD5 silencing resulted in a significant increase in cell adhesion as determined by the cell aggregation assay in A549 cells transfected with control or FXYD5-specific siRNA (Fig. 2A,B). To determine whether the effect of FXYD5 on cell adhesion was fully or partially mediated by disrupting the intercellular interaction between the Na,K-ATPase $\beta_1$ subunits, the cell aggregation assay was performed in the presence of a $\beta_1$-blocking antibody. As a control, we also performed the assay in the presence of an E-cadherin-blocking antibody. These antibodies have been previously reported to almost equally decrease the rate of cell contact formation between MDCK cells (Vagin et al., 2006). The presence of the $\beta_1$-blocking antibody fully prevented the increase in adhesion observed after silencing FXYD5, whereas the E-cadherin-blocking antibody slightly decreased cell aggregation in FXYD5-depleted cells (Fig. 2A). Neither antibody altered formation of aggregates in cells transfected with the control siRNA; a control antibody had no effect on cells transfected with either control or FXYD5-specific siRNA (Fig. 2A). Similar results were obtained when the aggregation assay was performed in $Ca^{2+}$-free medium (Fig. 2B). These results suggest that the presence of FXYD5 at the plasma membrane specifically prevents intercellular $\beta_1$–$\beta_1$ interactions, which might contribute to the decrease in adhesion between neighboring cells.

### Complex glycosylation of the Na,K-ATPase $\beta_1$ subunit does not play a role in the regulation of intercellular adhesion by FXYD5

It has been previously reported that FXYD5 decreases the amount of E-cadherin in selected cell lines (Ino et al., 2002). However, we did not observe any change in the amount of total or plasma membrane E-cadherin in A549 cells when FXYD5 was silenced (Fig. 3A). Similarly, silencing of FXYD5 did not alter the total amount of Na,K-ATPase $\alpha_1$ or $\beta_1$ subunit at the plasma membrane or in cell lysates (Fig. 3A). In A549 cell lysates, the Na,K-ATPase $\beta_1$ subunit was detected as two bands, whereas only the upper band was present in the plasma membrane. This band represents the $\beta_1$ subunit with complex-type *N*-glycans that are formed in the Golgi, whereas the lower band corresponds to the ER-resident fraction (Tokhtaeva et al., 2009). In agreement with previous reports (Lubarski et al., 2011), FXYD5 silencing decreased the electrophoretic mobility of the complex-type glycosylated $\beta_1$ subunit both at the plasma membrane and in cell lysates but did not alter the mobility of the ER-resident form (Fig. 3A). These results suggest that FXYD5 modifies the structure of the $\beta_1$ subunit complex-type *N*-glycans. FXYD5 silencing did not alter the electrophoretic mobility of E-cadherin or CD29 (Fig. 3A), suggesting that the effect of FXYD5 toward the $\beta_1$ subunit was specific.

To determine whether glycosylation of the $\beta_1$ subunit plays a role in the FXYD5 effect on intercellular adhesion, confluent MDCK-YFP–$\beta_1$ or MDCK cells expressing the unglycosylated $\beta_1$ subunit (MDCK-YFP–UG-$\beta_1$) were infected with Ad-Null or Ad-FXYD5. As expected, overexpression of Ad-FXYD5 decreased the ability of MDCK-YFP–$\beta_1$ cells to form junctions (Fig. 3B). Similarly, the prevention of *N*-glycosylation of the $\beta_1$ subunit delayed the formation of cell contacts, but to a lesser degree than FXYD5. With FXYD5 overexpression, the rate of contact formation was the same in MDCK-YFP–$\beta_1$ and MDCK-YFP–UG-$\beta_1$ cells, suggesting no contribution of the $\beta_1$ *N*-glycans to the anti-adhesive effects of FXYD5 (Fig. 3B). However, the possibility that FXYD5 affects cell adhesion by modifying the glycosylation of endogenous subunits in MDCK-YFP–UG-$\beta_1$ cells cannot be excluded. To alter glycosylation of all $\beta_1$ subunits, we used two inhibitors of *N*-glycan processing, an inhibitor of the Golgi mannosidase II called swainsonine, and a mannosidase I inhibitor called deoxymannojirimycin (DMM). The inhibitors, unlike mutations, preserve *N*-glycans in the $\beta_1$ subunit, but abolish the formation of complex-type chains in these *N*-glycans and hence are appropriate

Journal of Cell Science (2016) 129, 2394-2406 doi:10.1242/jcs.186148

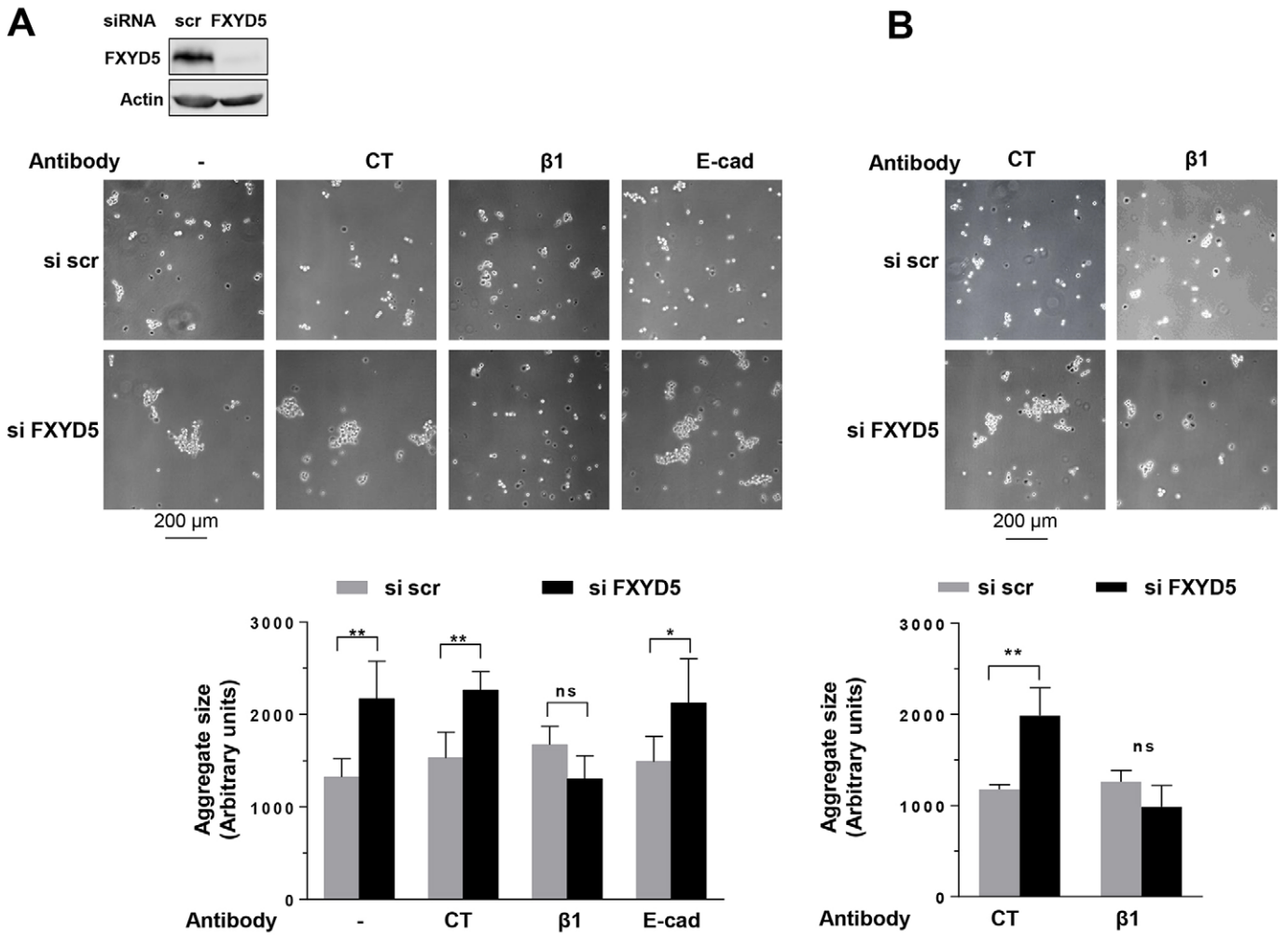


**Fig. 2. The increase in cell adhesion by FXYD5 knockdown is prevented by antibody specific to the Na,K-ATPase $\beta_1$ subunit.** (A) siRNA-transfected A549 cells were incubated in the presence or absence of a control (CT), Na,K-ATPase $\beta_1$ subunit ($\beta_1$) or E-cadherin (E-cad) antibody and the aggregation assay was performed as described. scr, scrambled siRNA. Results are mean±s.d. (*n*=4). A western blot showing FXYD5 silencing is also shown. (B) As in A, but the assay was performed in $Ca^{2+}$-free medium. Results are mean±s.d. (*n*=3). *$P \leq 0.05$; **$P \leq 0.01$; ns, not significant (one-way ANOVA and Sidak's multiple comparisons test).

tools to address the question of whether the FXYD5-mediated alteration of the $\beta_1$ subunit complex-type chains contributes to the effect of FXYD5 on cell adhesion. Both inhibitors prevented the effect of FXYD5 silencing on the size of the $\beta_1$ subunit *N*-glycans (Fig. 3C), but they did not affect the increase in cell adhesion by FXYD5 silencing (Fig. 3D). Taken together these results indicate that the effects of FXYD5 on the $\beta_1$ subunit *N*-glycans and intercellular adhesion are unrelated.

### Leu196, Glu197, Tyr199 and Tyr205 are crucial for the $\beta_1$–$\beta_1$ interaction and intercellular adhesion

The amino acid region downstream of the second *N*-glycosylation site, 193NES, in the Na,K-ATPase $\beta_1$ subunit is crucial for intercellular interactions between $\beta_1$ subunits (Tokhtaeva et al., 2011). The presence of the T202 residue in this region of the rat $\beta_1$ subunit (Fig. 4A, red arrow) is mostly responsible for the lack of interaction between rat and dog subunits (Tokhtaeva et al., 2012). Those results suggest that conserved residues both upstream and downstream of the 202 position are involved in homo-species $\beta_1$–$\beta_1$ interactions. To identify these residues, MDCK cell lines expressing the YFP–$\beta_1$ mutants with point mutations (L196A, E197A, Y199A or Y205A) or their combinations [L196A, E197A and Y199A (LEY/AAA), and L196A, E197A, Y199A and Y205A (LEYY/AAAA)] were created (Fig. 4A). All mutants were expressed at similar levels and predominantly localized in the lateral membrane as detected by confocal microscopy and by western blot analysis (Figs 4B and 5A, GFP blot). The levels of the endogenous $\beta_1$ subunit were also similar among all the cell lines (Fig. 5A, $\beta_1$ M17-P5-F11 and 464.8 blots). For better quantitative comparison of antibody signals, cell lysates were treated with PNGase F to deglycosylate the endogenous and exogenous $\beta_1$ subunits. All the point mutations resulted in a substantial decrease in the reactivity with the adhesion-blocking M17-P5-F11 $\beta_1$ antibody (Vagin et al., 2006) as compared with the wild-type YFP-$\beta_1$. Moreover, the Y199A and combined mutants were not recognized at all (Fig. 5A, M17-P5-F11 $\beta_1$ blot). The effect of these mutations on $\beta_1$–$\beta_1$ interactions was evaluated by immunoprecipitation of the YFP–$\beta_1$ subunit and analysis of the amount of co-immunoprecipitated endogenous $\beta_1$ by immunoblotting (Fig. 5B). This assay predominantly reflects the intercellular interactions between the exogenous and endogenous $\beta_1$ subunits (Tokhtaeva et al., 2011). The amount of co-immunoprecipitated endogenous $\beta_1$ was significantly decreased by all mutations with the Y199A mutation resulting in the strongest inhibition (Fig. 5B,C), indicating a crucial role of Y199 for $\beta_1$-$\beta_1$ interaction.

Journal of Cell Science (2016) 129, 2394-2406 doi:10.1242/jcs.186148

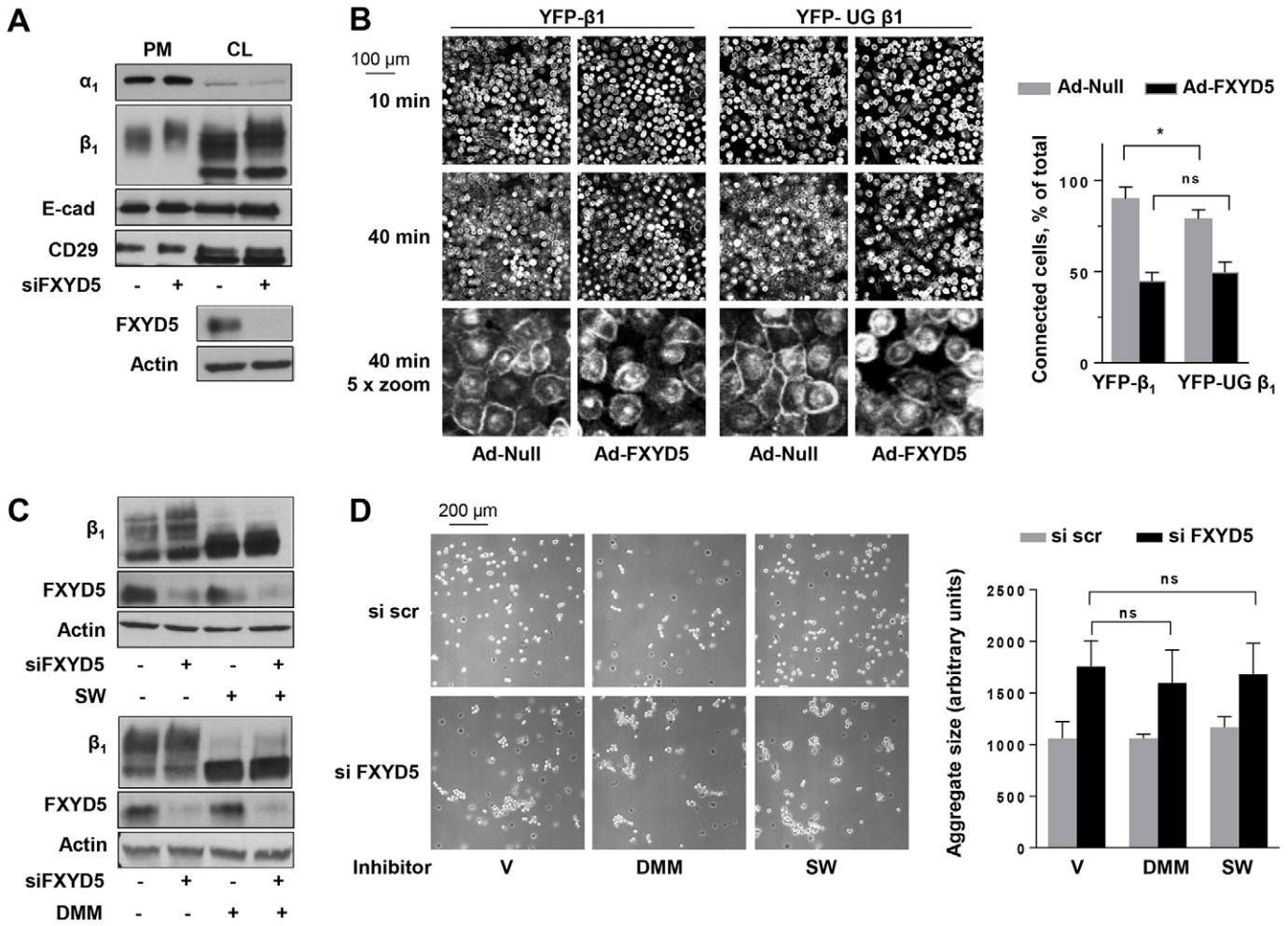


**Fig. 3. The increase in cell adhesion by silencing FXYD5 is not abolished by preventing complex glycosylation of the $\beta_1$ subunit.** (A) The levels of the Na,K-ATPase $\alpha_1$ and $\beta_1$ subunits, E-cadherin (E-cad), CD29, FXYD5 and actin were determined by western blotting of the plasma membrane (PM) and in cell lysate (CL) of A549 cells transfected with siRNA against FXYD5 (siFXYD5). *n*=3. (B) MDCK-YFP-$\beta_1$ or MDCK-YFP-UG-$\beta_1$ cells were infected with Ad-Null or Ad-FXYD5. The formation of intercellular contacts was assessed by confocal microscopy at the indicated time points after the intercellular junctions were disrupted by treatment with PBS. Representative images and quantification (mean±s.d., *n*=4) of the results are shown. (C,D) A549 cells were incubated with vehicle (V) or in the presence of 2 µg/ml swainsonine (SW) or 1 mM deoxymannojirimycin (DMM) and transfected with siRNA as indicated. Cell lysates were either analyzed by western blotting (C) or the cells were used in the aggregation assay (D). Representative images and quantification are shown. scr, scrambled siRNA. Results are mean±s.d. (*n*=4). *$P \leq 0.05$; ns, not significant (one-way ANOVA and Sidak's multiple comparisons test).

To determine whether this residue is also important for intercellular adhesion, the effects of the secreted protein containing the extracellular domain of the wild-type dog $\beta_1$ subunit (WT Sec-$\beta_1$) or its Y199A mutant (Y199A Sec-$\beta_1$) on the formation of cell contacts were compared. Surface-attached single MDCK cells were incubated in the presence or absence of WT or mutated Sec-$\beta_1$ in the medium in similar quantities as detected by western blotting (Fig. 6A). At the beginning of the assay, all cells had a round shape and did not have any contacts with each other. After 6 h of incubation in control medium, the majority of the cells formed cell–cell contacts (Fig. 6B, left panel). WT Sec-$\beta_1$, by competing with the $\beta_1$–$\beta_1$ interaction between neighboring cells, decreased the formation of cell–cell contacts, whereas the presence of Y199A Sec-$\beta_1$ did not have an effect (Fig. 6B, middle and right panels). The percentage of connected cells with the respective Sec-$\beta_1$ was time-dependent and significantly different from the untreated control for the WT Sec-$\beta_1$, but not for the Y199A Sec-$\beta_1$ (Fig. 6C). Taken together, these results suggest that the Y199 residue is required for $\beta_1$–$\beta_1$ interaction and intercellular adhesion.

### FXYD5 inhibits intercellular adhesion by impairing the amino-acid-mediated $\beta_1$-$\beta_1$ interaction

Primary rat ATII (rATII) cells were infected with Ad-Null (Vadasz et al., 2008), Ad-FXYD5 alone or in combination with the adenovirus encoding for YFP-linked wild-type (Ad-WT-YFP-$\beta_1$) or Y199A mutated (Ad-Y199A-YFP-$\beta_1$) rat Na,K-ATPase $\beta_1$ subunit. All the proteins were expressed at the plasma membrane of rATII cells as seen from confocal microscopy images taken ~40 h after infection (Fig. 7A). Similar to the endogenous form of FXYD5 in hATII and A549 cells, exogenous FXYD5 was detected by western blotting in two forms, the diffuse 70–75 kDa band, which presumably represents the plasma membrane form, and a sharper 50-kDa band corresponding to the protein core (Fig. 7B). Expression of YFP–$\beta_1$, both the wild-type and the mutated form, increased the levels of the endogenous $\alpha_1$ subunit (Fig. 7B), suggesting that additional $\beta_1$ subunits assemble with the excess of the $\alpha_1$ subunits and traffic to the plasma membrane. Overexpression of FXYD5 decreased trans-epithelial electrical resistance (TEER) of rATII cell monolayers. Infection with Ad-WT-YFP-$\beta_1$ did not

Journal of Cell Science (2016) 129, 2394-2406 doi:10.1242/jcs.186148

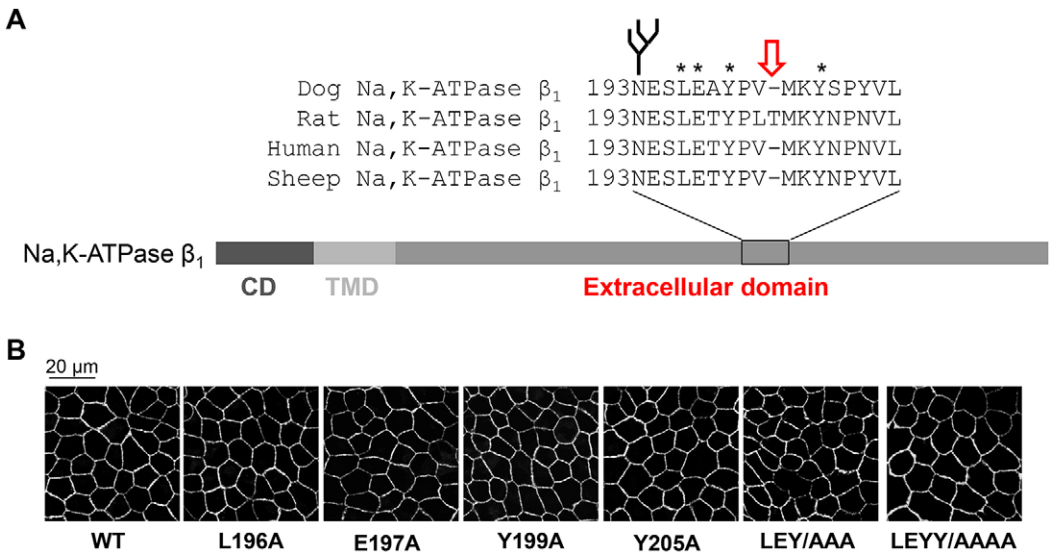


**Fig. 4. Mutations in the trans-dimerization domain do not affect the plasma membrane localization of the $\beta_1$ subunit.** (A) Protein sequence alignment of amino acid region from 193–210 of $\beta_1$ subunits from different species, showing the presence of T202 (red arrow) in the rat but not in dog, human or sheep sequences. The conserved residues mutated to alanine residues are indicated by stars. CD, cytoplasmic domain; TMD, transmembrane domain. (B) Confocal microscopy images of cell monolayers formed by stable MDCK cell lines expressing WT and mutated YFP-linked $\beta_1$ subunits.

significantly change the TEER as compared to cells infected with a null adenovirus (Fig. 7C). Expression of Ad-Y199A-YFP-$\beta_1$ alone decreased TEER (Fig. 7C), consistent with the impairment of $\beta_1$–$\beta_1$ interactions by the mutation (Fig. 5B,C). Co-expression of the wild-type YFP–$\beta_1$ with FXYD5 prevented the FXYD5-induced decrease in TEER, whereas the mutant had no effect (Fig. 7C). Both Na,K-ATPase $\alpha_1$ and $\beta_1$ subunits in rATII cells expressing mCherry–HA–FXYD5 were less resistant to the extraction with 0.25% Triton X-100 from cell monolayers than the proteins from cells infected with a null adenovirus (Fig. 7D). However, the expression of FXYD5 had no effect on the extraction of E-cadherin as compared with control rATII cells. These results suggest that FXYD5 specifically destabilizes the Na,K-ATPase at the intercellular junctions and decreases the tightness of epithelial junctions by disrupting the Y199-mediated $\beta_1$–$\beta_1$ bridges.

Damage of the alveolar capillary barrier results in the accumulation of fluid in the alveolar space (Dada and Sznajder, 2003). To study the effect of FXYD5 in a more physiological setting, we measured the concentration of proteins in bronchoalveolar lavage fluid (BALF) after infection of mice with control or FXYD5 adenovirus. At 72 h after intra-tracheal instillation of the adenovirus, there was an eightfold increase in FXYD5 mRNA in lung peripheral tissue compared to mice infected with null adenovirus. In agreement with this finding, the concentration of proteins in BALF was also increased, suggesting that the elevated levels of FXYD5 in the lung epithelium impair the epithelial barrier causing an influx of protein-rich fluid into the alveolar space.

### The inhibiting effect of FXYD5 on intercellular adhesion depends on the presence of *O*-glycans in its ectodomain

To determine the role of FXYD5 ectodomain in the impairment of intercellular adhesion, we designed several constructs encoding secreted variants of FXYD5 by removing the sequence corresponding to the cytosolic and transmembrane domains and inserting the HA tag in different locations. However, none of the constructs was expressed as detected by transient transfection of HEK-293 followed by western blot analysis of cell lysates and culture medium (data not shown). We reasoned that the presence of the transmembrane domain is essential for normal folding of the extracellular domain of FXYD5 during translation. As an alternative approach, we modified *O*-glycans in FXYD5 ectodomain by using the *O*-glycosylation inhibitor, benzyl-2-acetamido-2-deoxy-α-D-galactopyranoside (Benzyl-α-GalNAc) which blocks glycosyltransferase-mediated incorporation of glucosamine into *O*-glycans reducing the complexity of mucin-type *O*-glycans (Delannoy et al., 1996) or by mutagenic replacement of selected *O*-glycosylation sites in FXYD5.

Incubation of null-infected rATII or HGE-20 cells with Benzyl-α-GalNAc did not alter TEER, whereas, in Ad-FXYD5-infected cells the inhibitor prevented the decrease in TEER caused by FXYD5 overexpression (Fig. 8A,B). In both cell types, the inhibitor decreased the complexity of *O*-glycans linked to plasma membrane FXYD5 as evident from the increased electrophoretic mobility of mCherry–HA–FXYD5, but did not decrease the amount of protein (Fig. 8C). Moreover, in HGE-20 cells, cell incubation with Benzyl-α-GalNAc slightly increased the amount of mCherry–HA–FXYD5 in the plasma membrane (Fig. 8C). In either cell type, the inhibitor had no effect on the plasma membrane level of E-cadherin or the Na, K-ATPase $\alpha_1$ subunit (Fig. 8C). Importantly, the inhibitor increased TEER only in the presence of overexpressed FXYD5, pointing to the specific role of FXYD5 *O*-glycans in the disruption of intercellular junctions.

To further explore the role of FXYD5 *O*-glycans in intercellular adhesion, we determined the effect of partial prevention of FXYD5 *O*-glycosylation by mutagenesis of putative *O*-glycosylation sites on the ability of the cells to form colonies. HEK-293 cells were transfected with wild-type FXYD5 or its mutant with three putative *O*-glycosylation sites (T56, T57 and T62) replaced with alanine residues (TTT/AAA). At 24 h after transfection, cells were biotinylated and lysed, analyzed by confocal microscopy or fixed and stained with F-actin to visualize all cells. The mutation decreased FXYD5 surface expression (data not shown). When transfections were performed by adding double the amount of cDNA for TTT/AAA relative to the wild-type FXYD5 to sparsely plated single surface-attached cells, similar levels of wild-type FXYD5 and TTT/AAA were detected at the plasma membrane

Journal of Cell Science (2016) 129, 2394-2406 doi:10.1242/jcs.186148

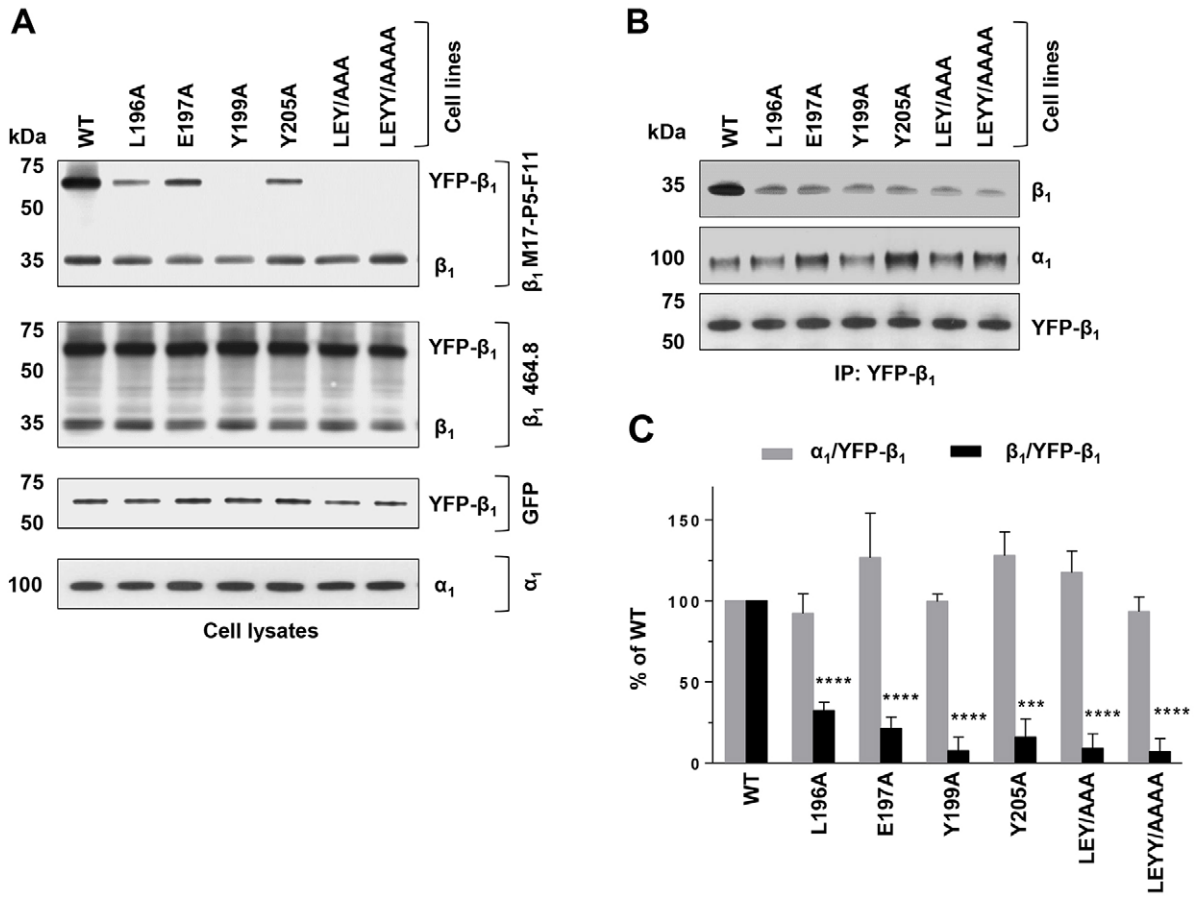


**Fig. 5. Tyrosine 199 is important for $\beta_1$–$\beta_1$ interaction.** (A) Equal amount of cell lysate protein from MDCK cells expressing the WT or mutated YFP–$\beta_1$ subunits was analyzed by western blotting with the indicated antibodies. (B) The exogenous YFP–$\beta_1$ subunits were immunoprecipitated using anti-GFP antibody, and YFP–$\beta_1$ and endogenous Na,K-ATPase $\alpha_1$ and $\beta_1$ subunits were analyzed by western blotting. (C) Densitometry analysis of the data presented in B was performed by normalizing the $\alpha_1$ and deglycosylated $\beta_1$ signals to deglycosylated YFP–$\beta_1$ signal. Results are mean±s.d. ($n$=3). ***$P$≤0.001; ****$P$≤0.0001 (significant difference from WT by Student's test).

by surface biotinylation (Fig. 8D) and confocal microscopy (Fig. 8E). The mutation increased the electrophoretic mobility of FXYD5 (Fig. 8D) indicating that at least some of the three sites are occupied by *O*-glycans in the wild-type protein. The mutation also increased the intracellular accumulation of FXYD5 (Fig. 8E). Imaging analysis of F-actin-stained transfected cells demonstrated that cells expressing TTT/AAA formed bigger colonies as compared to cells expressing the wild-type FXYD5 (Fig. 8F). Taken together, these results indicate that extensive *O*-glycosylation is responsible for the FXYD5-mediated disruptive effect on intercellular adhesion.

In conclusion, the results demonstrate that the *O*-glycosylated ectodomain of FXYD5 impairs the epithelial junctions by interfering with intercellular Na,K-ATPase trans-dimerization without affecting the expression or stability of E-cadherin at the plasma membrane.

## DISCUSSION

The Na,K-ATPase heterodimer facilitates cell–cell interactions by undergoing intercellular trans-dimerization through the extracellular 197–208 amino-acid region of its $\beta_1$ subunit (Tokhtaeva et al., 2012). In contrast, little is known about the mechanism involved in the disruption of cell junctions by FXYD5. FXYD5 is expressed in normal and cancer cells (Gabrielli et al., 2011; Ino et al., 2002; Lee et al., 2012; Lubarski et al., 2005; Maehata et al., 2011; Mitselou et al., 2010; Park et al., 2011; Shimada et al., 2004). In normal cells, FXYD5 increases the Na,K-ATPase activity (Lubarski et al., 2005). This increase in the Na,K-ATPase activity due to the elevated expression of FXYD5 in airway epithelia results in deleterious effects in patients with cystic fibrosis (Miller and Davis, 2008), whereas such an increase in muscles is thought to provide a compensatory mechanism for the decrease in the α–β $Na^+$ pump in patients with chronic spinal cord injury (Boon et al., 2012). In different cancer types, high FXYD5 expression has been described as a predictor of metastasis and poor prognosis (Batistatou et al., 2007b; Ino et al., 2002; Shimamura et al., 2004; Tamura et al., 2005). Several lines of evidence presented here indicate that the *O*-glycosylated extracellular domain of FXYD5 impairs epithelial adhesion by steric hindrance of the intercellular interactions between the key amino acid residues responsible for $\beta_1$–$\beta_1$ binding, including Y199. In cancer cells that have a high level of both expression and *O*-glycosylation of FXYD5, the increase in cell adhesiveness caused by silencing FXYD5 is prevented specifically by an antibody against Na,K-ATPase $\beta_1$ subunit. In normal epithelial cells, the anti-adhesive effect of FXYD5 is partially prevented by increasing the number of $\alpha_1\beta_1$ heterodimers following the overexpression of the wild-type $\beta_1$ subunit, whereas overexpression of the mutant that is unable to form $\beta_1$–$\beta_1$ bridges has no protective effect. The disruptive effect of FXYD5 on cell adhesion is abolished by genetic or pharmacological inhibition of FXYD5 *O*-glycosylation.

Journal of Cell Science (2016) 129, 2394-2406 doi:10.1242/jcs.186148

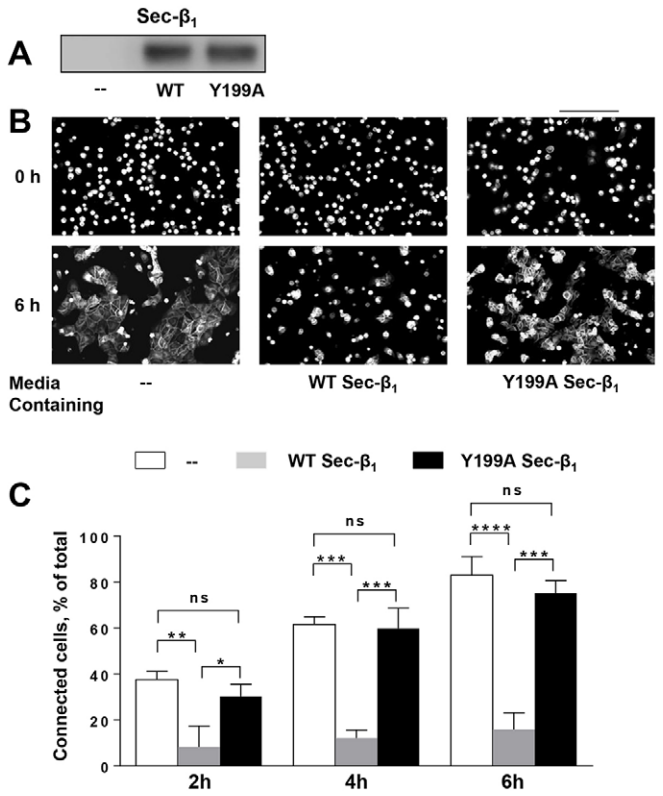


**Fig. 6. Tyrosine 199 is important for cell adhesion.** (A) Western blot analysis of culture medium from HEK-293 cells either non-transfected or transfected with WT Sec-$\beta_1$ or Y199A Sec-$\beta_1$. The 464.8 antibody that reacts with both the WT and Y199A $\beta_1$ subunit was used. (B,C) MDCK cells were plated sparsely and the formation of intercellular contacts was monitored by confocal microscopy (B) and the percentage of connected cells was calculated (C). Results are mean±s.d. ($n$=3). *$P$≤0.05; **$P$≤0.01; ***$P$≤0.001; ****$P$≤0.0001; ns, not significant (one-way ANOVA and Tukey's multiple comparisons test).

Previous studies based on the reported differences in size (~50–55 kDa in cancer cells and ~24 kDa in normal tissues) have suggested that FXYD5 is extensively *O*-glycosylated in cancer cells but has very few carbohydrate residues in normal tissues (Ino et al., 2002; Lubarski et al., 2011, 2007). Contrary to this, FXYD5 has been detected as a ~90-kDa protein in normal human testes (Gabrielli et al., 2011). The data presented here demonstrate that FXYD5 is extensively *O*-glycosylated both in cancer and normal cells. Furthermore, our data suggest that the discrepancies on the molecular mass of FXYD5 between different reports might be a consequence of using antibodies with different specificities toward unglycosylated and glycosylated forms of FXYD5. The two FXYD5-specific antibodies used here recognize a core (or slightly *O*-glycosylated) intracellular form of about 32 kDa, but not the plasmalemma-resident form of FXYD5. The recognition of this extensively *O*-glycosylated form is enabled by the partial removal of *O*-glycans with glycosidases.

Our data show that only the extensively *O*-glycosylated forms of FXYD5 are present at the plasma membrane, which implies that *O*-glycosylation is important for surface expression of FXYD5. In support of such interpretation, the lack of selected *O*-glycans in FXYD5 as a result of *O*-glycosylation site mutations decreases the surface amount of FXYD5 relative to its intracellular content. Notably, the surface expression of FXYD5 is not decreased by cell exposure to the inhibitor of *O*-glycosylation, which does not prevent the attachment of *O*-glycans to FXYD5 but decreases them in size. Taken together, these results indicate that the presence of whole *O*-glycans attached to FXYD5 ectodomain is required for plasma membrane targeting and stable surface expression of the protein.

Overexpression of FXYD5 increases cell motility, impairs cell adhesion and promotes experimental cancer metastasis (Ino et al., 2002; Nam et al., 2007; Shimada et al., 2004; Shimamura et al., 2004). In agreement with this, our data show that FXYD5 silencing in cancer cells ameliorates adhesion whereas FXYD5 overexpression in normal epithelial cells impairs it. Infection of mice with FXYD5 adenovirus increases lung permeability which is in agreement with a recent report on the increased expression of FXYD5 in the lungs of patients with acute respiratory distress syndrome, a syndrome characterized by interstitial edema and severe alveolar epithelial damage (Wujak et al., 2016). Moreover, we demonstrate that the anti-adhesive effect of FXYD5 depends on the presence of *O*-glycans in its extracellular domain. This conclusion is in contrast with previously published data showing that expression of FXYD5, but not of the chimera consisting of the intracellular and transmembrane domains of FXYD4 and the extracellular domain of FXYD5 decreased trans-epithelial resistance in M1 epithelial cell monolayers (Lubarski et al., 2007). However, no evidence was presented on the plasma membrane localization of the expressed proteins in M1 cells, which makes the interpretation of the results unclear. Our data show that the decrease in the number of *O*-glycans in FXYD5 ectodomain by the mutagenic replacement of selected *O*-glycosylation sites increases the ability of cells to form intercellular contacts. Furthermore, we demonstrate that the inhibitor of *O*-glycosylation Benzyl-α-GalNAc decreases the complexity of *O*-glycans in the plasmalemma-resident FXYD5 and protects the tight junctions from the FXYD5-induced disruption without decreasing the surface amount of the protein. These data do not agree with previous reports on a decrease in FXYD5 expression without changes in its molecular mass in Benzyl-α-GalNAc-exposed cells (Tsuiji et al., 2003), which was interpreted by the authors as an accelerated degradation of FXYD5. Considering our data, we propose that the loss of FXYD5 detection observed in the inhibitor-treated cells (Tsuiji et al., 2003) was due to the reduced affinity of the antibody binding to the less glycosylated forms of the protein.

The mutation of L196, E197, Y199 or Y205 disrupts intercellular $\beta_1$–$\beta_1$ interactions and the recognition by the adhesion-blocking antibody. The Y199 mutation has the greatest effect on both parameters and also inhibits intercellular adhesion. In normal epithelial cells, overexpression of the wild-type $\beta_1$ subunits rescues the tight junctions from the effect of FXYD5, whereas overexpression of the Y199 mutant does not. The rescue of FXYD5-impaired TEER by $\beta_1$ overexpression is in agreement with previous results showing that overexpression of the Na,K-ATPase $\beta_1$ subunit in the alveolar epithelium improves lung liquid clearance in rats (Factor et al., 1998). Given that the effects of FXYD5 depend on the presence of Y199 in the Na,K-ATPase $\beta_1$ subunit, the plausible interpretation is that the bulky *O*-glycosylated ectodomain of FXYD5 prevents $\beta_1$–$\beta_1$ interactions by steric hindrance. In agreement with previous publications (Lubarski et al., 2011), silencing of FXYD5 alters the size of complex-type *N*-glycans in the plasma membrane Na,K-ATPase $\beta_1$ subunit in A549 cells. However, the FXYD5-knockdown-induced increase in cell adhesion was not blocked by using inhibitors that prevent the formation of complex-type *N*-glycans, indicating that the effects of FXYD5 on the intercellular adhesion are not mediated through the changes in $\beta_1$ subunit glycosylation. The effect of FXYD5 on the size of $\beta_1$ subunit *N*-glycans seems to be specific for the $\beta_1$ subunit

Journal of Cell Science (2016) 129, 2394-2406 doi:10.1242/jcs.186148

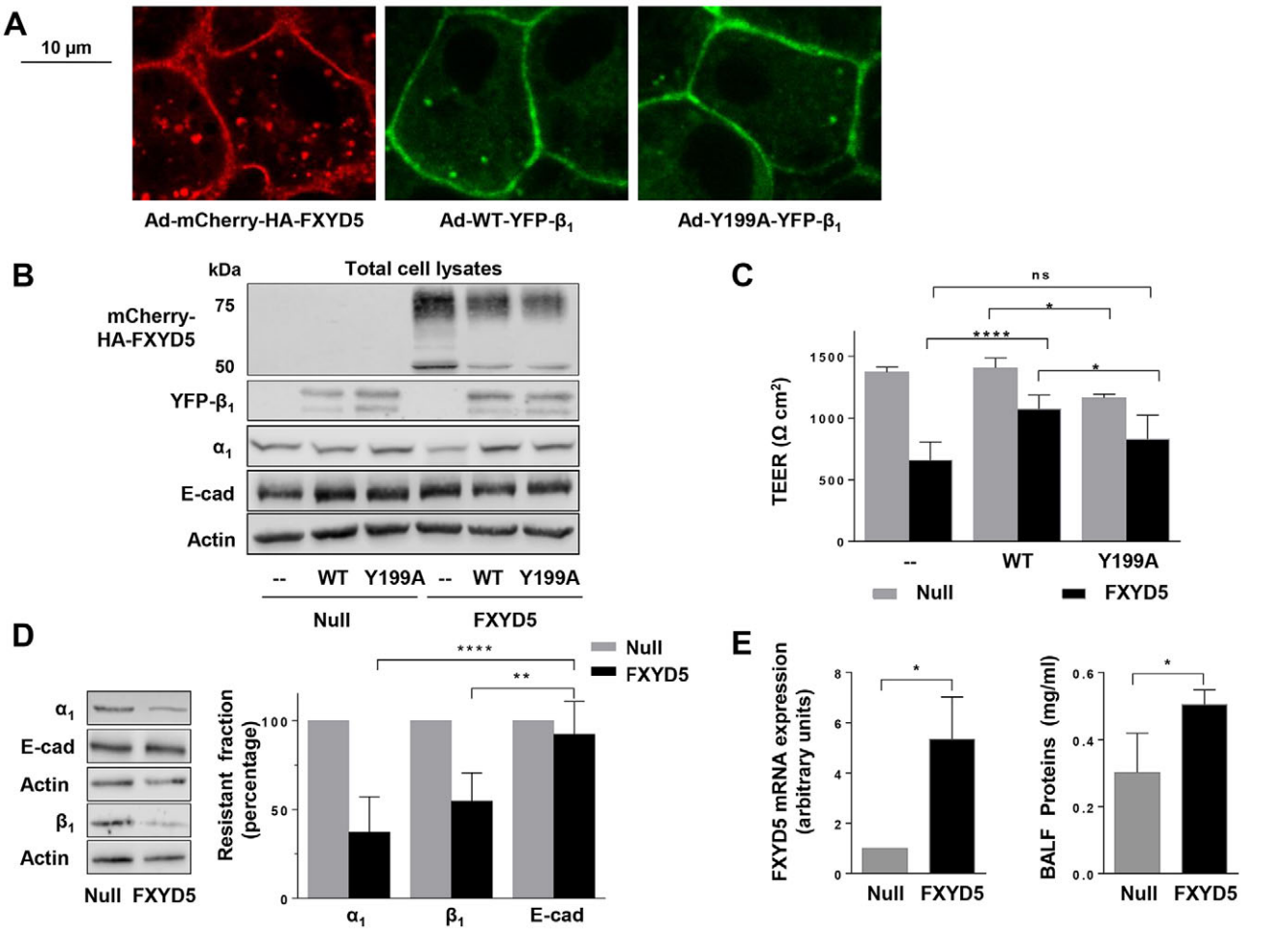


**Fig. 7. The disruptive effect of FXYD5 on the tight junctions is prevented by overexpression of the Na,K-ATPase $\beta_1$ subunit.** (A) rATII cells were infected with Ad-mCherry-HA-FXYD5, Ad-WT-YFP-$\beta_1$ or Ad-Y199-YFP-$\beta_1$ and analyzed by confocal microscopy. Representative images are shown. (B) rATII cells were infected with either Ad-Null or Ad-mCherry-HA-FXYD5 in the absence or presence of Ad-WT-YFP-$\beta_1$ or Ad-Y199-YFP-$\beta_1$. Na,K-ATPase $\alpha_1$ and $\beta_1$ (YFP-$\beta_1$), E-cadherin (E-cad), FXYD5 (mCherry-HA-FXYD5) levels were determined by western blotting in total cell lysates. $n$=4. (C) rATII cells were infected as in B and the TEER was determined. Results are mean±s.d. ($n$=6). *$P$≤0.05; ****$P$≤0.0001; ns, not significant (one-way ANOVA and Sidak's multiple comparisons test). (D) rATII cells were infected with Ad-Null or Ad-FXYD5. Cells were treated with 0.25% Triton X-100 in PBS for 15 min, the solution was discarded and the cells lysed. The levels of $\alpha_1$, deglycosylated $\beta_1$ and E-cadherin were determined by western blotting. Bars represent the mean±s.d. fraction resistant to treatment with 0.25% Triton X-100 ($n$=6). **$P$≤0.01, ****$P$≤0.0001 (one-way ANOVA and Sidak's multiple comparisons test). (E) Mice were instilled with Ad-Null or Ad-FXYD5. At 72 h after infection FXYD5 mRNA and protein concentration were determined in lung peripheral tissue or BALF, respectively. Results are mean±s.d. ($n$=3). *$P$≤0.05 (Student's $t$-test).

as neither E-cadherin nor CD29 glycosylated forms were modified. The data suggest that the close proximity of a large *O*-glycosylated ectodomain of FXYD5 limits the accessibility of the $\beta_1$ subunit *N*-glycans to Golgi glycosyltransferases, resulting in a decreased number of residues added to the complex-type carbohydrate chains in these *N*-glycans. Such interpretation is consistent with our conclusion on the interference of the *O*-glycosylated extracellular domain of FXYD5 with $\beta_1$–$\beta_1$ interactions.

In many tumor tissues, the protein level of FXYD5 inversely correlates with the level of E-cadherin (Batistatou et al., 2008; Maehata et al., 2011; Mitselou et al., 2010; Ono et al., 2010; Shimada et al., 2004); however, whether this is a result of FXYD5-induced downregulation of E-cadherin is unknown. Overexpression of FXYD5 reduced the levels of E-cadherin in particular cell lines (Ino et al., 2002), but had no effect in others (Lubarski et al., 2011). Silencing of FXYD5 in a number of cancer cell lines did not alter the levels of E-cadherin and the effects of FXYD5 on cell invasiveness were observed in an E-cadherin-lacking cell line (Nam et al., 2006; Shimamura et al., 2004). The results presented here demonstrate that transient FXYD5 overexpression or silencing in several normal and cancer epithelial cells does affect the intercellular adhesion but does not alter the level of E-cadherin. Taken together, these data further support the existence of E-cadherin-independent mechanisms of the FXYD5-induced impairment of cell–cell adhesion.

Therefore, the role of the Na,K-ATPase in regulating intercellular adhesion is complex. Whereas the $\alpha_1$–$\beta_1$ heterodimer acts as a cell adhesion molecule and contributes to the formation and stabilization of junctions, FXYD5 impairs cell adhesion. The results presented here indicate that the prevalent effect of the Na,K-ATPase on cell adhesion depends on the quantity of FXYD5 relative to that of the $\alpha_1$–$\beta_1$ heterodimers (Fig. 8G). Moreover, we show the importance of extensive *O*-glycosylation for the anti-adhesive effect of FXYD5.

## MATERIALS AND METHODS

### Reagents

Chemical and cell culture reagents were purchased from Sigma-Aldrich (St Louis, MO) or Corning Life Sciences (Tewksbury, MA), and Cellgro Mediatech, (Manassas, VA), respectively, unless stated otherwise.

Journal of Cell Science (2016) 129, 2394-2406 doi:10.1242/jcs.186148

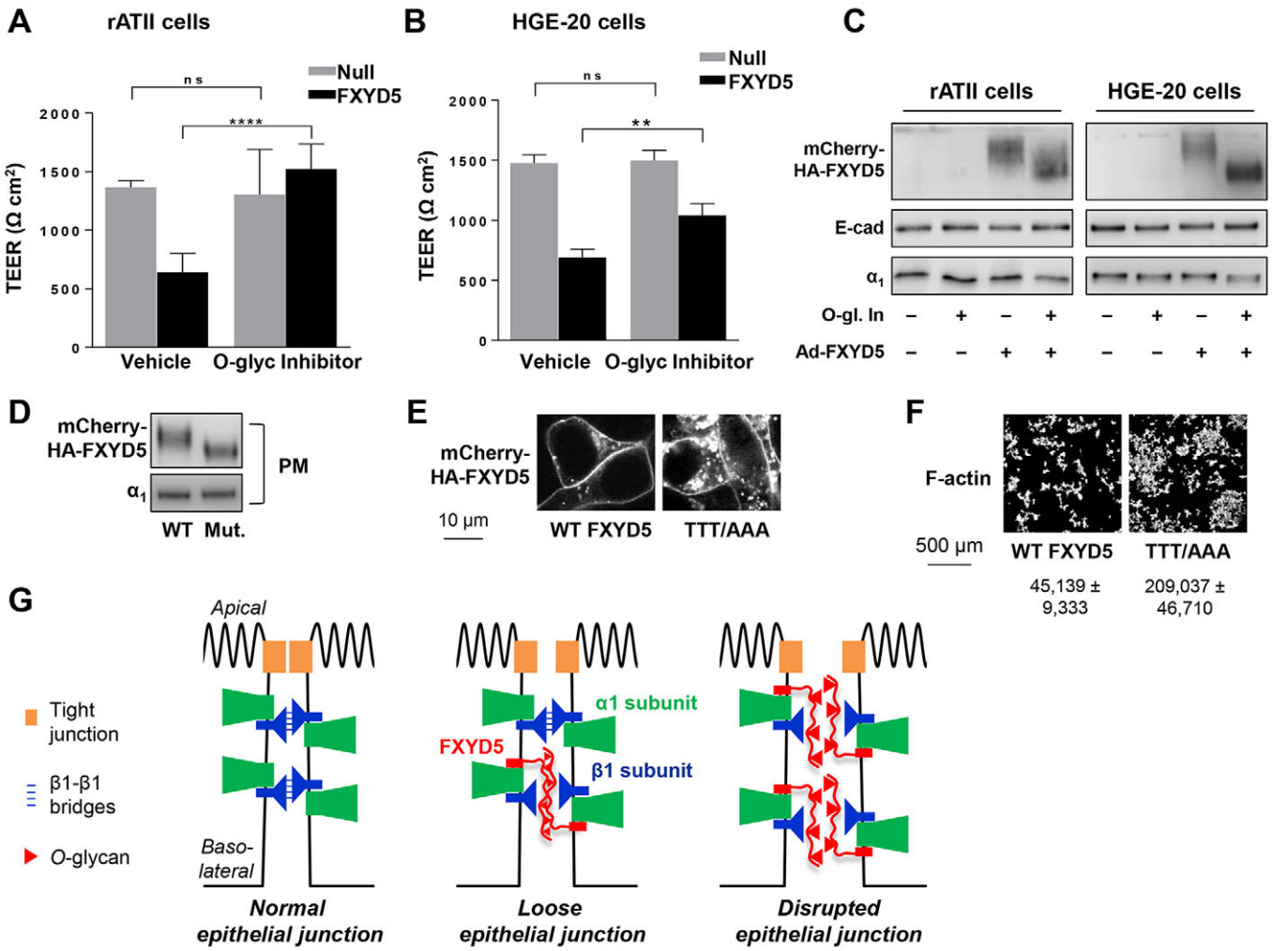


**Fig. 8. The disruptive effect of FXYD5 on the tight junctions is prevented by inhibiting FXYD5 *O*-glycosylation.** rATII or HGE-20 cells were infected with Ad-Null or Ad-FXYD5 followed by adding benzyl-α-GalNAc (O-glyc inhibitor; 1.6 mM). (A,B) The TEER was determined. Results are mean±s.d. ($n$=6). $^{**}P \leq 0.01$; $^{****}P \leq 0.0001$; ns, not significant (one-way ANOVA and Sidak's multiple comparisons test). (C) The levels of FXYD5 (mCherry–HA–FXYD5), the Na,K-ATPase $\alpha_1$ subunit and E-cadherin (E-cad) at the plasma membrane were determined by western blotting. Representative blots are shown. $n$=4. (D–F) HEK-293 cells transfected with the wild-type mCherry-HA-FXYD5 or its T56A, T57A and T62A triple mutant (mut. or TTT/AAA) were analyzed by surface biotinylation followed by western blot analysis (D), confocal microscopy (E) or fluorescent staining of actin filaments followed by confocal microscopy (F). Numbers below images refer to the average colony size in $\mu m^2$ [mean±s.d., $n$=3; $P$=0.002 (Student's $t$-test)]. PM, plasma membrane. (G) Cartoon depicting a complex role of the Na,K-ATPase in regulating adhesion. The prevalent effect of the Na,K-ATPase on cell adhesion depends on the ratio between FXYD5 and the $\alpha_1$–$\beta_1$ heterodimers and on the extent of FXYD5 *O*-glycosylation.

### Cell culture

MDCK, HEK-293, HGE-20 and A549 cells (ATCC, Manassas, VA) and A549-GFP-$\alpha_1$ contamination free were grown and maintained as previously described (Chailler and Ménard, 2005; Dada et al., 2003; Vagin et al., 2006).

### Generation of mCherry–HA–FXYD5 cDNA

pIRES-HYG-FXYD5 [a gift of Haim Garty, Department of Biological Chemistry, The Weizman Institute of Science, Rehovot, Israel (Lubarski et al., 2011)] was used as a source for FXYD5 cDNA, and pReceiver-M56 (GeneCopoeia, Inc., Rockville, MD) was used as a source of cDNA for mCherry. A PCR fragment coding for the N-terminal signal peptide of mouse FXYD5 followed by HA tag, a PCR fragment coding for the rest of FXYD5 and a PCR fragment coding for mCherry were cloned using a GeneArt Seamless Cloning and Assembly Kit (Invitrogen, Carlsbad, CA) into pIRES, resulting in the sequence coding for FXYD5 with HA–mCherry fused between the signal peptide and the extracellular domain.

### Adenoviral infection

Mice and rats were provided with food and water *ad libitum*, maintained on a 14-h-light–10-h-dark cycle, and handled according to National Institutes of Health guidelines and an experimental protocol approved by the Northwestern University Institutional Animal Care and Use Committee. ATII cells were isolated from the lungs of male Sprague-Dawley rats by elastase digestion and culture in DMEM (Vagin et al., 2005; Ridge et al., 2003). The day of isolation and plating of rATII on transwell inserts was designated day 0. All experiments were conducted on day 3. Where indicated, cells were treated with 0.25% Triton X-100 in PBS, which was removed and discarded after 15 min incubation on ice followed by cell lysis (Vagin et al., 2006).

To generate Ad-mCherry-HA-FXYD5, Ad-WT-YFP-$\beta_1$ and Ad-Y199A-YFP-$\beta_1$, the sequence encoding mCherry–HA–FXYD5, or the wild-type YFP-linked rat Na,K-ATPase $\beta_1$-subunit (Vagin et al., 2005), or its Y199A mutant were cloned into pVQAd CMV K-NpA (ViraQuest, Inc., North Liberty, IA) using a GeneArt Seamless Cloning and Assembly Kit (Invitrogen, Carlsbad, CA). Adenoviral production was performed by Viraquest, which provided viral titers and excluded wild-type viral contamination of the viral vectors (negative PCR for glycoprotein E1). Ad-Null was purchased from Viraquest.

Cells were infected with 20 plaque-forming units (pfu)/cell control adenovirus (Ad-null) or with Ad-FXYD5, Ad-WT-YFP-$\beta_1$, Ad-Y199A-YFP-$\beta_1$ or their combination as previously described (Vadasz et al., 2008). TEER was measured using EVOM Epithelial Voltohmmeter (World

Journal of Cell Science (2016) 129, 2394-2406 doi:10.1242/jcs.186148

Precision Instruments, Sarasota, FL). The inhibitor of *O*-glycosylation Benzyl-α-GalNAc (1.6 mM) was added at 30 h and 48 h prior to TEER measurements in rATII and HGE-20 cells, respectively.

Mice at 8–12 weeks of age were infected with adenoviral vectors ($1\times10^9$ pfu/animal) in 50% surfactant vehicle as previously described (Mutlu et al., 2004) and housed in a barrier facility for 72 h. After 72 h BALF was obtained through a 20-gauge angiocath ligated into the trachea through a tracheostomy. A total of 1-ml of PBS was instilled into the lungs and then aspirated three times. BALF was centrifuged to remove cells and used to determine proteins (Urich et al., 2011). RNA was isolated from lungs using an RNeasy kit (QIAGEN, Valencia, CA) and reverse transcribed using qScript cDNA synthesis (Quanta Biosciences, Gaithersburg, MD, USA). Quantitative PCRs were set up using iQ SYBR Green Super mix (Bio Rad, Hercules, CA). Data were normalized to the abundance of L19 mRNA. The primers for FXYD5 and L19 were: FXYD5, 5′-CATCCTACATTGAACA-TCCA-3′ and 5′-TGAGACAACTGCCTACAC-3′ and L19, 5′-AGCCTG-TGACTGTCCATTC-3′ and 5′-ATCCTCATCCTTCTCATCCAG-3′.

### Human subjects

Studies using human subjects were approved by the Northwestern University Institutional Review Board (Chicago, IL; STU00041428-MODCR0003). De-identified human lung tissue obtained from donors whose lungs were unsuitable for transplantation was provided by the National Disease Research Interchange (NRDI). We do not have any contact with the subject and other than the disease state of the lung we do not receive any information on the subjects that could allow us to identify the donor directly or indirectly. Human ATII cells were isolated using a modification of the methods previously described (Kim et al., 2014).

### Mutagenesis and construction of stable cell lines

Mutants of Sec-$\beta_1$, mCherry–HA–FXYD5 and YFP–$\beta_1$ were constructed by site-directed mutagenesis using the QuikChange mutagenesis kit (Agilent Technologies, Santa Clara, CA). Stable MDCK cell lines expressing the wild-type and mutated YFP–$\beta_1$ were obtained as described previously (Vagin et al., 2006).

### Primary antibodies and western blot analysis

The following monoclonal antibodies were used: GFP, clones 7.1 and 13.1, which also recognize YFP (dilution 1:1000; cat. no. 11814460001; Roche Diagnostics, Indianapolis, IN), Na,K-ATPase α1 subunit, clone C464.6 (dilution 1:2000; cat. no. 05-369; EMD Millipore, MA), Na,K-ATPase β1 subunit, clone M17-P5-F11 (dilution 1:1000; cat. no. MA3-930; Affinity Bioreagents, Golden, CO), Na,K-ATPase β1 subunit, clone 464.8 (dilution 1:1000; cat. no. NB300-147; Novus Biologicals, Littleton, CO), β1-integrin/CD29 (dilution 1:1000; cat. no. 610467; BD Transduction Laboratories, CA), Dysadherin, clone D-2 (dilution 1:500; cat. no. sc-166782; Santa Cruz Biotechnology, Inc., Santa Cruz, CA), E-cadherin, clone 36 (dilution 1:1000; cat. no. 610181; BD Biosciences), HA (clone 16B12; dilution 1:1000; cat. no. 901502; Biolegend, San Diego, CA, USA) and HA, clone F-7 (dilution 1:500; cat. no. sc-7392; Santa Cruz Biotechnology). The following polyclonal antibodies were used: FXYD5 (dilution 1:1000; cat. no. HPA010817; Sigma-Aldrich), Na,K-ATPase $\beta_1$ subunit (dilution 1:1000; cat. no. GTX113390; GeneTex, Irvine, CA) which was used to detect the $\beta_1$ subunit after PNGase F treatment in rATII cells, and β-actin (dilution 1:1000; cat. no. 4967; Cell Signaling, Danvers, MA). SDS-PAGE and western blot analysis was performed as described previously (Tokhtaeva et al., 2012). Incubation with primary antibodies was performed overnight at 4°C. Immunoblots were quantified by densitometry using Image J 1.46r (National Institutes of Health, Bethesda, MD) or Image Studio Software (LI-COR Inc., Lincoln, NE). Where indicated, cell lysates were treated by PNGase F from *Flavobacterium meningosepticum* or *O*-glycosidase & Neauraminidase Bundle according to the manufacturer's instructions (New England Biolabs Inc., Ipswich, MA, USA) prior to loading on SDS-PAGE.

### Immunoprecipitation

YFP-linked $\beta_1$ subunits were immunoprecipitated from MDCK cell lysates using polyclonal antibodies against GFP and YFP (Clontech, Mountain View, CA) as described previously (Tokhtaeva et al., 2012). To enable quantitative comparison of immunoprecipitated YFP-linked and co-precipitated endogenous $\beta_1$ subunits, the bead-adherent proteins were deglycosylated by using PNGase F from *Flavobacterium meningosepticum* (New England BioLabs, Ipswich, MA) (Tokhtaeva et al., 2012). Proteins eluted from the beads were separated by SDS-PAGE and analyzed by western blotting.

### Surface-specific biotinylation

Biotinylation and isolation of surface proteins was performed according to previously described procedures (Dada et al., 2012; Gottardi et al., 1995; Vagin et al., 2006) using EZ-Link™ Sulfo-NHS-SS-biotin and streptavidin beads (Thermo Scientific Pierce Protein Biology, Rockford, IL). Where indicated, the streptavidin bead-adherent proteins were treated with *O*-glycosidase & Neuraminidase Bundle (New England BioLabs) as described by the manufacturer and analyzed by western blotting.

### siRNA and cDNA transfection

A549 cells were transfected with 120 pmol of human FXYD5 siRNA duplex (final concentration 100 µM) (Santa Cruz Biotechnology) using Lipofectamine RNAiMAX (Invitrogen). A non-silencing negative control siRNA was purchased from Life Technologies. HEK-293 cells were transfected with vectors encoding the wild-type or TTT/AAA mutated mCherry–HA–FXYD5 using Lipofectamine-2000 (Invitrogen). Experiments were performed 24 h after transfection.

### Production of secreted proteins

WT Sec–$\beta_1$ or Y199A Sec–$\beta_1$ was expressed in HEK-293 cells by transient transfection using Lipofectamine-2000. The medium was changed 6 h after transfection, and the medium containing Sec–$\beta_1$ was collected 48 h later.

### Cell aggregation assay for A549 cells

Cell aggregation was assessed by a hanging drop assay that was performed as previously described (Qin et al., 2005; Tokhtaeva et al., 2012). Cell suspensions containing $2.5\times10^4$ cells in 40 µl of cell culture medium with or without 20 µg/ml anti-$\beta_1$ antibody (clone M17-P5-F11), anti-E-cadherin mouse monoclonal antibody (clone DECMA-1; EMD Millipore) and an IgG1K control antibody (EMD Millipore), were placed as drops on the lid of a 35-mm culture plate and processed as previously described (Tokhtaeva et al., 2012). After incubation cell aggregates in each drop were subjected to shear force by passage through a 200-µl wide-bore pipette tip to disperse loosely associated cells and photographed using a Nikon Eclipse TE200 inverted microscope (Nikon Metrology, Brighton, MI, USA) using a 10× phase-contrast objective. Aggregates were traced and the aggregate area was measured using MetaMorph Software (Molecular Devices, Sunnyvale, CA). For the $Ca^{2+}$-free experiments the medium contained: 150 mM NaCl, 5 mM KCl, 1 mM $MgCl_2$, 10 mM glucose, 25 mM sodium bicarbonate and 0.25 mM EGTA pH 7.4 (Gusarova et al., 2011).

### Cell adhesion assay for MDCK cells

Confluent MDCK-YFP-$\beta_1$ or MDCK-YFP-UG-$\beta_1$ cells grown on collagen-coated glass-bottom microwell dishes (MatTek Corporation, Ashland, MA) were infected with Ad-null or Ad-mCherry-HA-FXYD5 as described above. After removing the culture medium, cells were rinsed twice and incubated for 1 h with $Ca^{2+}$-free PBS to disrupt cell contacts. Then PBS was replaced with $Ca^{2+}$-containing culture medium, and the re-formation of cell–cell contacts was monitored by acquiring images of the same fields on microwell dishes at 10 and 40 min after adding the medium.

To study the effect of Sec-$\beta_1$ on the formation of cell contacts between MDCK cells, MDCK cells expressing a YFP-linked plasma membrane marker (NTCP–YFP, Vagin et al., 2006) were trypsinized and sparsely plated on collagen-coated glass-bottom microwell dishes. After the majority of cells attached to the glass, non-adherent cells were removed by rinsing, and fresh medium with or without WT Sec-$\beta_1$ or Y199A Sec-$\beta_1$ was added to the cells. The formation of cell–cell contacts was monitored by acquiring images of the same fields on microwell dishes every 2 h. Cell–cell adhesion was quantified by calculating the percentage of cells that did form contacts with the neighboring cells at the indicated time intervals of incubation.

### Fluorescent staining and confocal microscopy and image analysis

Actin filaments were visualized in fixed MDCK or HEK-293 cells using Alexa-Fluor-633–phalloidin (Thermo Fisher Scientific) as described previously (Vagin et al., 2006). Confocal microscopy images were acquired using a Zeiss LSM 510 laser scanning confocal microscope (Carl Zeiss MicroImaging GmbH, Germany). Colony size was measured using ZEN 2009 software (Carl Zeiss MicroImaging). 10–12 microscopic fields were analyzed for each condition.

### Statistical analysis

Data are expressed as mean±s.d. For comparisons between two groups, significance was evaluated by Student's *t*-test, and when more than two groups were compared, one-way ANOVA was used followed by the Tukey or Sidak test using GraphPad Prism 6.07 software.

#### Acknowledgements

The authors dedicate this paper to the memory of Haim Garty whose work on FXYD5 inspired the present study. We thank Erin Hogan for the isolation of rATII cells, Liora Shoshani for providing the Sec-$\beta_1$ plasmid and Daniel Mènard for allowing use of HGE-20 cells for this work.

#### Competing interests

The authors declare no competing or financial interests.

#### Author contributions

E.T., H.S., N.D.-Y., Y.W., N.M.G., K.M.R., P.N.S. and E.A.M. performed experiments, M.V.-L. assisted with the research design and data analysis, G.S., E.A.M. and J.I.S. discussed and edited the manuscript, O.V. and L.A.D. designed the research, performed experiments, analyzed data and wrote the manuscript.

#### Funding

This work was supported, in part, by the National Institutes of Health [grant numbers R37-HL48129 to J.I.S., HL071643 to J.I.S., K.M.R. and L.A.D., HL113350 to L.A.D. and O.V., USVA 2I01BX001006 to G.S., DK105156-01 to G.S., PICT_SU1072 to M.V.-L., K08DK100661 to E.A.M.]; and the UCLA Children's Discovery and Innovation Institute (to E.A.M.). Deposited in PMC for release after 12 months.

#### References

**Balasubramaniam, S. L., Gopalakrishnapillai, A. and Barwe, S. P.** (2015). Ion dependence of Na-K-ATPase-mediated epithelial cell adhesion and migration. *Am. J. Physiol. Cell Physiol.* **309**, C437-C441.

**Barwe, S. P., Kim, S., Rajasekaran, S. A., Bowie, J. U. and Rajasekaran, A. K.** (2007). Janus model of the Na,K-ATPase beta-subunit transmembrane domain: distinct faces mediate alpha/beta assembly and beta-beta homo-oligomerization. *J. Mol. Biol.* **365**, 706-714.

**Barwe, S. P., Skay, A., McSpadden, R., Huynh, T. P., Langhans, S. A., Inge, L. J. and Rajasekaran, A. K.** (2012). Na,K-ATPase beta-subunit cis homo-oligomerization is necessary for epithelial lumen formation in mammalian cells. *J. Cell Sci.* **125**, 5711-5720.

**Batistatou, A., Makrydimas, G., Zagorianakou, N., Zagorianakou, P., Nakanishi, Y., Agnantis, N. J., Hirohashi, S. and Charalabopoulos, K.** (2007a). Expression of dysadherin and E-cadherin in trophoblastic tissue in normal and abnormal pregnancies. *Placenta* **28**, 590-592.

**Batistatou, A., Peschos, D., Tsanou, H., Charalabopoulos, A., Nakanishi, Y., Hirohashi, S., Agnantis, N. J. and Charalabopoulos, K.** (2007b). In breast carcinoma dysadherin expression is correlated with invasiveness but not with E-cadherin. *Br. J. Cancer* **96**, 1404-1408.

**Batistatou, A., Charalabopoulos, K., Nakanishi, Y., Vagianos, C., Hirohashi, S., Agnantis, N. J. and Scopa, C. D.** (2008). Differential expression of dysadherin in papillary thyroid carcinoma and microcarcinoma: correlation with E-cadherin. *Endocr. Pathol.* **19**, 197-202.

**Bertorello, A. M., Komarova, Y., Smith, K., Leibiger, I. B., Efendiev, R., Pedemonte, C. H., Borisy, G. and Sznajder, J. I.** (2003). Analysis of Na+, K+-ATPase motion and incorporation into the plasma membrane in response to G protein-coupled receptor signals in living cells. *Mol. Biol. Cell* **14**, 1149-1157.

**Boon, H., Kostovski, E., Pirkmajer, S., Song, M., Lubarski, I., Iversen, P. O., Hjeltnes, N., Widegren, U. and Chibalin, A. V.** (2012). Influence of chronic and acute spinal cord injury on skeletal muscle Na+-K+-ATPase and phospholemman expression in humans. *Am. J. Physiol. Endocrinol. Metab.* **302**, E864-E871.

**Cereijido, M., Contreras, R. G., Shoshani, L. and Larre, I.** (2012). The Na+-K+-ATPase as self-adhesion molecule and hormone receptor. *Am. J. Physiol. Cell Physiol.* **302**, C473-C481.

**Chailler, P. and Ménard, D.** (2005). Establishment of human gastric epithelial (HGE) cell lines exhibiting barrier function, progenitor, and prezymogenic characteristics. *J. Cell Physiol.* **202**, 263-274.

**Clément, M., Rocher, J., Loirand, G. and Le Pendu, J.** (2004). Expression of sialyl-Tn epitopes on beta1 integrin alters epithelial cell phenotype, proliferation and haptotaxis. *J. Cell Sci.* **117**, 5059-5069.

**Clifford, R. J. and Kaplan, J. H.** (2008). beta-Subunit overexpression alters the stoicheometry of assembled Na-K-ATPase subunits in MDCK cells. *Am. J. Physiol. Renal Physiol.* **295**, F1314-F1323.

**Dada, L. A. and Sznajder, J. I.** (2003). Mechanisms of pulmonary edema clearance during acute hypoxemic respiratory failure: role of the Na,K-ATPase. *Crit. Care Med.* **31**, S248-S252.

**Dada, L. A., Chandel, N. S., Ridge, K. M., Pedemonte, C., Bertorello, A. M. and Sznajder, J. I.** (2003). Hypoxia-induced endocytosis of Na,K-ATPase in alveolar epithelial cells is mediated by mitochondrial reactive oxygen species and PKC-ζ. *J. Clin. Invest.* **111**, 1057-1064.

**Dada, L., Gonzalez, A. R., Urich, D., Soberanes, S., Manghi, T. S., Chiarella, S. E., Chandel, N. S., Budinger, G. R. S. and Mutlu, G. M.** (2012). Alcohol worsens acute lung injury by inhibiting alveolar sodium transport through the adenosine A1 receptor. *PLoS ONE* **7**, e30448.

**Delannoy, P., Kim, I., Emery, N., De Bolos, C., Verbert, A., Degand, P. and Huet, G.** (1996). Benzyl-N-acetyl-alpha-D-galactosaminide inhibits the sialylation and the secretion of mucins by a mucin secreting HT-29 cell subpopulation. *Glycoconj. J.* **13**, 717-726.

**Factor, P., Saldias, F., Ridge, K., Dumasius, V., Zabner, J., Jaffe, H. A., Blanco, G., Barnard, M., Mercer, R., Perrin, R. et al.** (1998). Augmentation of lung liquid clearance via adenovirus-mediated transfer of a Na,K-ATPase beta1 subunit gene. *J. Clin. Invest.* **102**, 1421-1430.

**Fujikura, Y., Krijt, J. and Nečas, E.** (2011). Liver and muscle hemojuvelin are differently glycosylated. *BMC Biochem.* **12**, 52.

**Gabrielli, N. M., Veiga, M. F., Matos, M. L., Quintana, S., Chemes, H., Blanco, G. and Vazquez-Levin, M. H.** (2011). Expression of dysadherin in the human male reproductive tract and in spermatozoa. *Fertil. Steril.* **96**, 554-561.e2.

**Garty, H. and Karlish, S. J. D.** (2006). Role of FXYD proteins in ion transport. *Annu. Rev. Physiol.* **68**, 431-459.

**Geering, K.** (2001). The functional role of beta subunits in oligomeric P-type ATPases. *J. Bioenerg. Biomembr.* **33**, 425-438.

**Geering, K.** (2006). FXYD proteins: new regulators of Na-K-ATPase. *Am. J. Physiol. Renal Physiol.* **290**, F241-F250.

**Gottardi, C. J., Dunbar, L. A. and Caplan, M. J.** (1995). Biotinylation and assessment of membrane polarity: caveats and methodological concerns. *Am. J. Physiol.* **268**, F285-F295.

**Gusarova, G. A., Trejo, H. E., Dada, L. A., Briva, A., Welch, L. C., Hamanaka, R. B., Mutlu, G. M., Chandel, N. S., Prakriya, M. and Sznajder, J. I.** (2011). Hypoxia leads to Na,K-ATPase downregulation via Ca(2+) release-activated Ca(2+) channels and AMPK activation. *Mol. Cell. Biol.* **31**, 3546-3556.

**Ino, Y., Gotoh, M., Sakamoto, M., Tsukagoshi, K. and Hirohashi, S.** (2002). Dysadherin, a cancer-associated cell membrane glycoprotein, down-regulates E-cadherin and promotes metastasis. *Proc. Natl. Acad. Sci. USA* **99**, 365-370.

**Kim, S.-J., Cheresh, P., Williams, D., Cheng, Y., Ridge, K., Schumacker, P. T., Weitzman, S., Bohr, V. A. and Kamp, D. W.** (2014). Mitochondria-targeted Ogg1 and aconitase-2 prevent oxidant-induced mitochondrial DNA damage in alveolar epithelial cells. *J. Biol. Chem.* **289**, 6165-6176.

**Lecuona, E., Dada, L. A., Sun, H., Butti, M. L., Zhou, G., Chew, T.-L. and Sznajder, J. I.** (2006). Na,K-ATPase {alpha}1-subunit dephosphorylation by protein phosphatase 2A is necessary for its recruitment to the plasma membrane. *FASEB J.* **20**, 2618-2620.

**Lee, S. H., Hatakeyama, S., Yu, S.-Y., Bao, X., Ohyama, C., Khoo, K.-H., Fukuda, M. N. and Fukuda, M.** (2009). Core3 O-glycan synthase suppresses tumor formation and metastasis of prostate carcinoma PC3 and LNCaP cells through down-regulation of alpha2beta1 integrin complex. *J. Biol. Chem.* **284**, 17157-17169.

**Lee, Y.-K., Lee, S.-Y., Park, J.-R., Kim, R.-J., Kim, S.-R., Roh, K.-J. and Nam, J.-S.** (2012). Dysadherin expression promotes the motility and survival of human breast cancer cells by AKT activation. *Cancer Sci.* **103**, 1280-1289.

**Lieber, M., Smith, B., Szakal, A., Nelson-Rees, W. and Todaro, G.** (1976). A continuous tumor-cell line from a human lung carcinoma with properties of type II alveolar epithelial cells. *Int. J. Cancer* **17**, 62-70.

**Lubarski, I., Pihakaski-Maunsbach, K., Karlish, S. J., Maunsbach, A. B. and Garty, H.** (2005). Interaction with the Na,K-ATPase and tissue distribution of FXYD5 (related to ion channel). *J. Biol. Chem.* **280**, 37717-37724.

**Lubarski, I., Karlish, S. J. D. and Garty, H.** (2007). Structural and functional interactions between FXYD5 and the Na+-K+-ATPase. *Am. J. Physiol. Renal Physiol.* **293**, F1818-F1826.

**Lubarski, I., Asher, C. and Garty, H.** (2011). FXYD5 (dysadherin) regulates the paracellular permeability in cultured kidney collecting duct cells. *Am. J. Physiol. Renal Physiol.* **301**, F1270-F1280.

**Maehata, Y., Hirahashi, M., Aishima, S., Kishimoto, J., Hirohashi, S., Yao, T., Takashima, H., Tsuneyoshi, M. and Oda, Y.** (2011). Significance of dysadherin

and E-cadherin expression in differentiated-type gastric carcinoma with submucosal invasion. *Hum. Pathol.* **42**, 558-567.

**Miller, T. J. and Davis, P. B.** (2008). FXYD5 modulates Na+ absorption and is increased in cystic fibrosis airway epithelia. *Am. J. Physiol. Lung Cell. Mol. Physiol.* **294**, L654-L664.

**Mitselou, A., Batistatou, A., Nakanishi, Y., Hirohashi, S., Vougiouklakis, T. and Charalabopoulos, K.** (2010). Comparison of the dysadherin and E-cadherin expression in primary lung cancer and metastatic sites. *Histol. Histopathol.* **25**, 1257-1267.

**Mutlu, G. M. and Sznajder, J. I.** (2005). Mechanisms of pulmonary edema clearance. *Am. J. Physiol. Lung Cell Mol. Physiol.* **289**, L685-L695.

**Mutlu, G. M., Dumasius, V., Burhop, J., McShane, P. J., Meng, F. J., Welch, L., Dumasius, A., Mohebahmadi, N., Thakuria, G., Hardiman, K. et al.** (2004). Upregulation of alveolar epithelial active Na+ transport is dependent on beta2-adrenergic receptor signaling. *Circ. Res.* **94**, 1091-1100.

**Nam, J.-S., Kang, M.-J., Suchar, A. M., Shimamura, T., Kohn, E. A., Michalowska, A. M., Jordan, V. C., Hirohashi, S. and Wakefield, L. M.** (2006). Chemokine (C-C motif) ligand 2 mediates the prometastatic effect of dysadherin in human breast cancer cells. *Cancer Res.* **66**, 7176-7184.

**Nam, J.-S., Hirohashi, S. and Wakefield, L. M.** (2007). Dysadherin: a new player in cancer progression. *Cancer Lett.* **255**, 161-169.

**Ono, K., Uramoto, H. and Hanagiri, T.** (2010). Expression of dysadherin and cytokeratin as prognostic indicators of disease-free survival in patients with stage I NSCLC. *Anticancer Res.* **30**, 3273-3278.

**Park, J.-R., Kim, R.-J., Lee, Y.-K., Kim, S.-R., Roh, K.-J., Oh, S. H., Kong, G., Kang, K.-S. and Nam, J.-S.** (2011). Dysadherin can enhance tumorigenesis by conferring properties of stem-like cells to hepatocellular carcinoma cells. *J. Hepatol.* **54**, 122-131.

**Qin, Y., Capaldo, C., Gumbiner, B. M. and Macara, I. G.** (2005). The mammalian Scribble polarity protein regulates epithelial cell adhesion and migration through E-cadherin. *J. Cell Biol.* **171**, 1061-1071.

**Rajasekaran, S. A. and Rajasekaran, A. K.** (2009). Na,K-ATPase and epithelial tight junctions. *Front. Biosci.* **14**, 2130-2148.

**Rajasekaran, S. A., Palmer, L. G., Moon, S. Y., Peralta Soler, A., Apodaca, G. L., Harper, J. F., Zheng, Y. and Rajasekaran, A. K.** (2001). Na,K-ATPase activity is required for formation of tight junctions, desmosomes, and induction of polarity in epithelial cells. *Mol. Biol. Cell* **12**, 3717-3732.

**Ridge, K. M., Olivera, W. G., Saldias, F., Azzam, Z., Horowitz, S., Rutschman, D. H., Dumasius, V., Factor, P. and Sznajder, J. I.** (2003). Alveolar type 1 cells express the alpha2 Na,K-ATPase, which contributes to lung liquid clearance. *Circ. Res.* **92**, 453-460.

**Shimada, Y., Yamasaki, S., Hashimoto, Y., Ito, T., Kawamura, J.-i., Soma, T., Ino, Y., Nakanishi, Y., Sakamoto, M., Hirohashi, S. et al.** (2004). Clinical significance of dysadherin expression in gastric cancer patients. *Clin. Cancer Res.* **10**, 2818-2823.

**Shimamura, T., Yasuda, J., Ino, Y., Gotoh, M., Tsuchiya, A., Nakajima, A., Sakamoto, M., Kanai, Y. and Hirohashi, S.** (2004). Dysadherin expression facilitates cell motility and metastatic potential of human pancreatic cancer cells. *Cancer Res.* **64**, 6989-6995.

**Shoshani, L., Contreras, R. G., Roldán, M. L., Moreno, J., Lázaro, A., Balda, M. S., Matter, K. and Cereijido, M.** (2005). The polarized expression of Na+,K+-ATPase in epithelia depends on the association between beta-subunits located in neighboring cells. *Mol. Biol. Cell* **16**, 1071-1081.

**Stamatovic, S. M., Keep, R. F., Wang, M. M., Jankovic, I. and Andjelkovic, A. V.** (2009). Caveolae-mediated internalization of occludin and claudin-5 during CCL2-induced tight junction remodeling in brain endothelial cells. *J. Biol. Chem.* **284**, 19053-19066.

**Sweadner, K. J. and Rael, E.** (2000). The FXYD gene family of small ion transport regulators or channels: cDNA sequence, protein signature sequence, and expression. *Genomics* **68**, 41-56.

**Sznajder, J. I.** (2001). Alveolar edema must be cleared for the acute respiratory distress syndrome patient to survive. *Am. J. Respir. Crit. Care Med.* **163**, 1293-1294.

**Tamura, M., Ohta, Y., Tsunezuka, Y., Matsumoto, I., Kawakami, K., Oda, M. and Watanabe, G.** (2005). Prognostic significance of dysadherin expression in patients with non–small cell lung cancer. *J. Thorac. Cardiovasc. Surg.* **130**, 740-745.

**Tokhtaeva, E., Sachs, G. and Vagin, O.** (2009). Assembly with the Na,K-ATPase alpha(1) subunit is required for export of beta(1) and beta(2) subunits from the endoplasmic reticulum. *Biochemistry* **48**, 11421-11431.

**Tokhtaeva, E., Sachs, G., Souda, P., Bassilian, S., Whitelegge, J. P., Shoshani, L. and Vagin, O.** (2011). Epithelial junctions depend on intercellular trans-interactions between the Na,K-ATPase beta subunits. *J. Biol. Chem.* **286**, 25801-25812.

**Tokhtaeva, E., Sachs, G., Sun, H., Dada, L. A., Sznajder, J. I. and Vagin, O.** (2012). Identification of the amino acid region involved in the intercellular interaction between the beta1 subunits of Na+/K+-ATPase. *J. Cell Sci.* **125**, 1605-1616.

**Tsuiji, H., Takasaki, S., Sakamoto, M., Irimura, T. and Hirohashi, S.** (2003). Aberrant O-glycosylation inhibits stable expression of dysadherin, a carcinoma-associated antigen, and facilitates cell-cell adhesion. *Glycobiology* **13**, 521-527.

**Urich, D., Eisenberg, J. L., Hamill, K. J., Takawira, D., Chiarella, S. E., Soberanes, S., Gonzalez, A., Koentgen, F., Manghi, T., Hopkinson, S. B. et al.** (2011). Lung-specific loss of the laminin alpha3 subunit confers resistance to mechanical injury. *J. Cell Sci.* **124**, 2927-2937.

**Vádasz, I., Raviv, S. and Sznajder, J. I.** (2007). Alveolar epithelium and Na,K-ATPase in acute lung injury. *Intensive Care Med.* **33**, 1243-1251.

**Vadasz, I., Dada, L. A., Briva, A., Trejo, H. E., Welch, L. C., Chen, J., Toth, P. T., Lecuona, E., Witters, L. A., Schumacker, P. T. et al.** (2008). AMP-activated protein kinase regulates CO2-induced alveolar epithelial dysfunction in rats and human cells by promoting Na,K-ATPase endocytosis. *J. Clin. Invest.* **118**, 752-762.

**Vagin, O., Tokhtaeva, E. and Sachs, G.** (2006). The role of the beta1 subunit of the Na,K-ATPase and its glycosylation in cell-cell adhesion. *J. Biol. Chem.* **281**, 39573-39587.

**Vagin, O., Tokhtaeva, E., Yakubov, I., Shevchenko, E. and Sachs, G.** (2008). Inverse correlation between the extent of N-glycan branching and intercellular adhesion in epithelia: contribution of the Na,K-ATPase beta1 subunit. *J. Biol. Chem.* **283**, 2192-2202.

**Vagin, O., Turdikulova, S. and Sachs, G.** (2005). Recombinant addition of N-glycosylation sites to Na,K-ATPase beta 1 subunit results in its clustering in caveolae and apical sorting in HGT-1 cells. *J. Biol. Chem.* 43159-43167.

**Vagin, O., Dada, L. A., Tokhtaeva, E. and Sachs, G.** (2012). The Na,K-ATPase alpha1beta1 heterodimer as a cell adhesion molecule in epithelia. *Am. J. Physiol. Cell Physiol.* **302**, C1271-C1281.

**Wujak, Ł. A., Blume, A., Baloğlu, E., Wygrecka, M., Wygowski, J., Herold, S., Mayer, K., Vadász, I., Besuch, P., Mairbäurl, H. et al.** (2016). FXYD1 negatively regulates Na+/K+-ATPase activity in lung alveolar epithelial cells. *Respir. Physiol. Neurobiol.* **220**, 54-61.